Electronic Supplementary Material (ESI) for Journal of Materials Chemistry A.
This journal is © The Royal Society of Chemistry 2018

Supplementary Information

Maximization of the Energy Capability Level in Transition Metal Complexes through Application of 1-Amino- and 2-Amino-5*H*-tetrazole Ligands

Norbert Szimhardt,[a] Maximilian H. H. Wurzenberger,[a] Lukas Zeisel,[a] Michael S. Gruhne,[a] Marcus Lommel[a] and Jörg Stierstorfer*[a]

[a] Department of Chemistry, Ludwig-Maximilian University of Munich, Butenandtstr. 5-13, D-81377 Munich, Germany.

Dr. Jörg Stierstorfer, jstch@cup.uni-muenchen.de, FAX +49 89 2180 77007

Table of Contents

1. Compounds overview

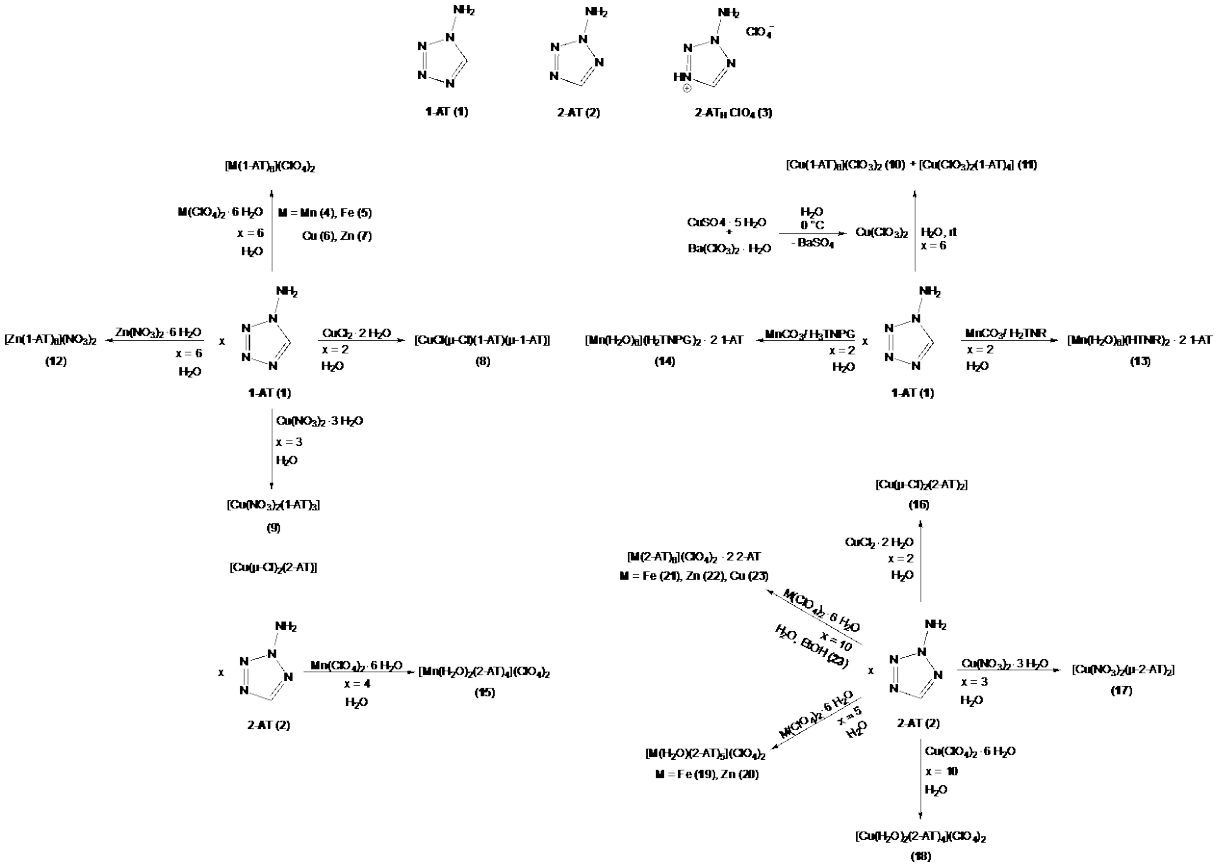

2. IR spectroscopy of 1–9, 12 and 16–23

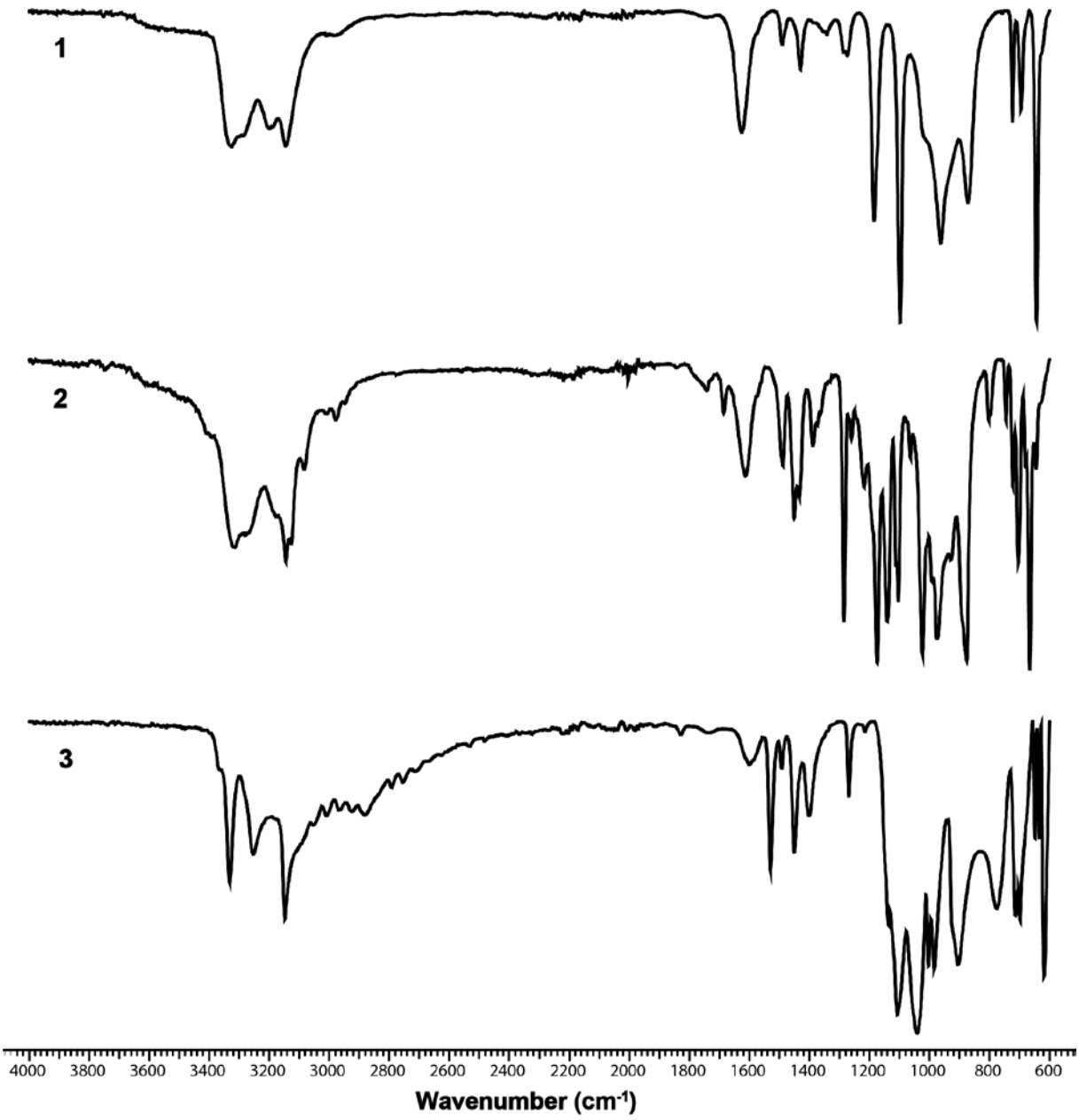

Figure S1 Infrared spectra of nitrogen-rich compounds **1**–**3**.

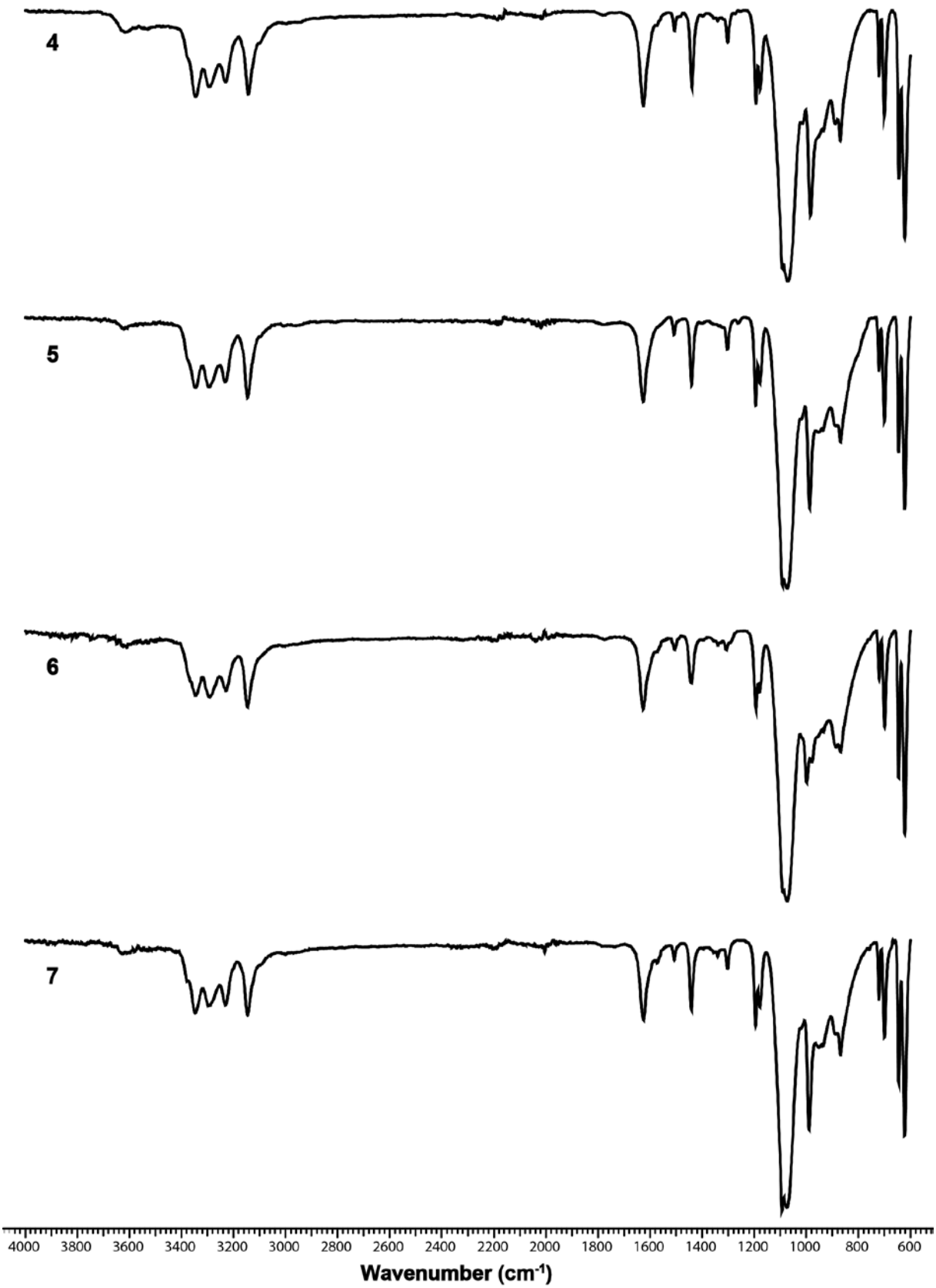

Figure S2 IR spectra of **4**–**7**.

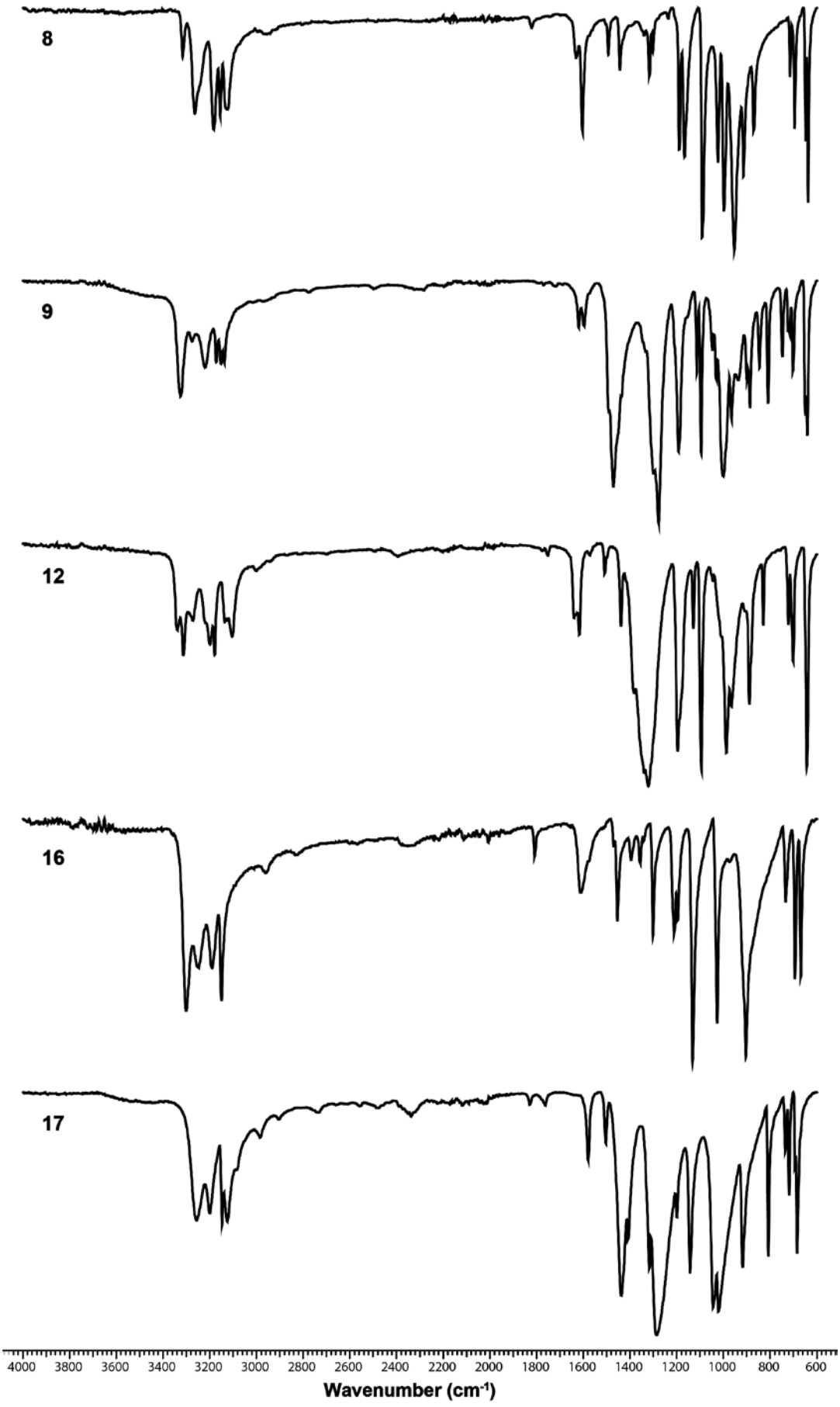

Figure S3 Infrared spectra of **8**, **9**, **12**, **16**, and **17**.

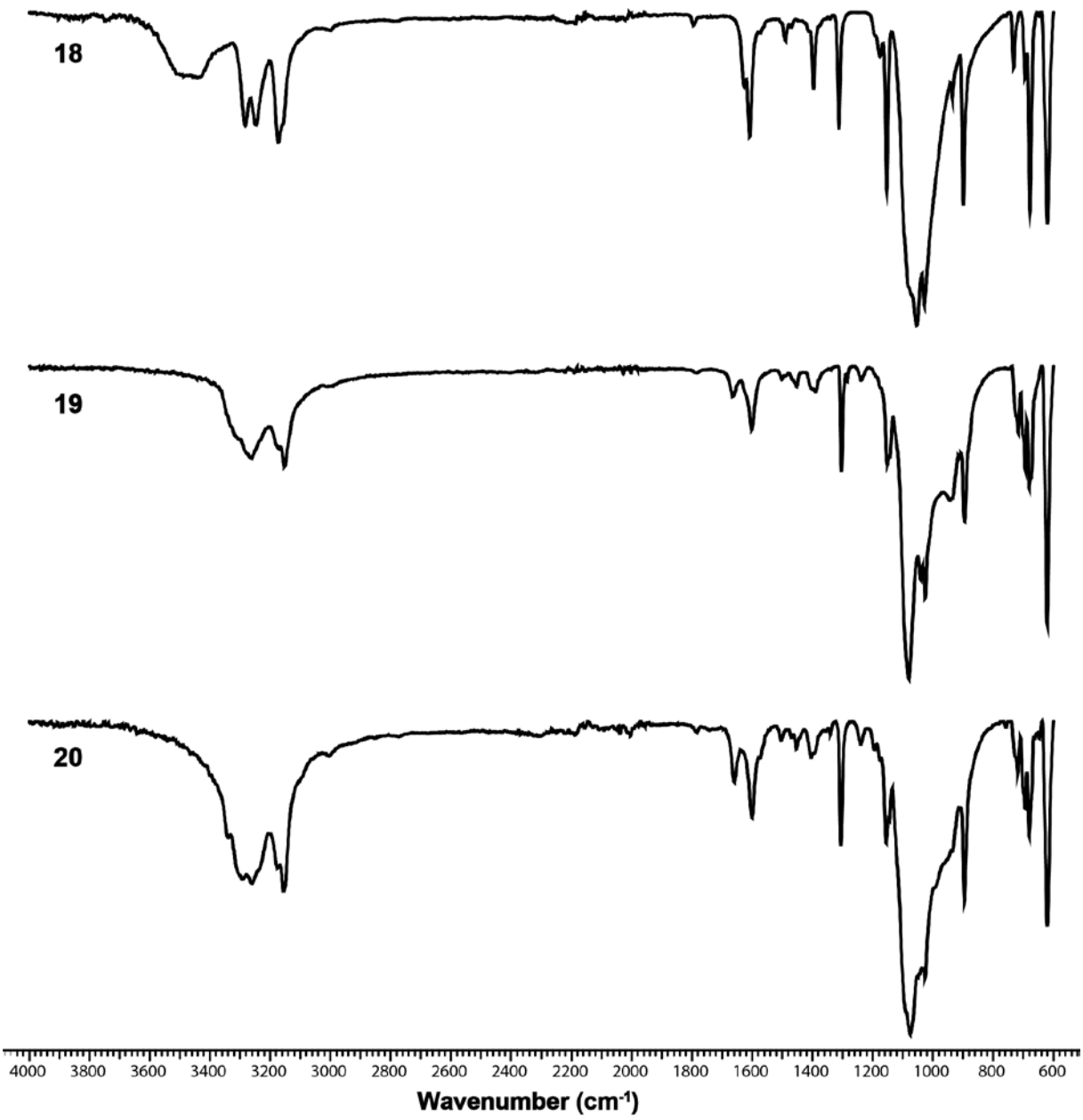

Figure S4 Infrared spectra of coordination compounds **18**–**20**.

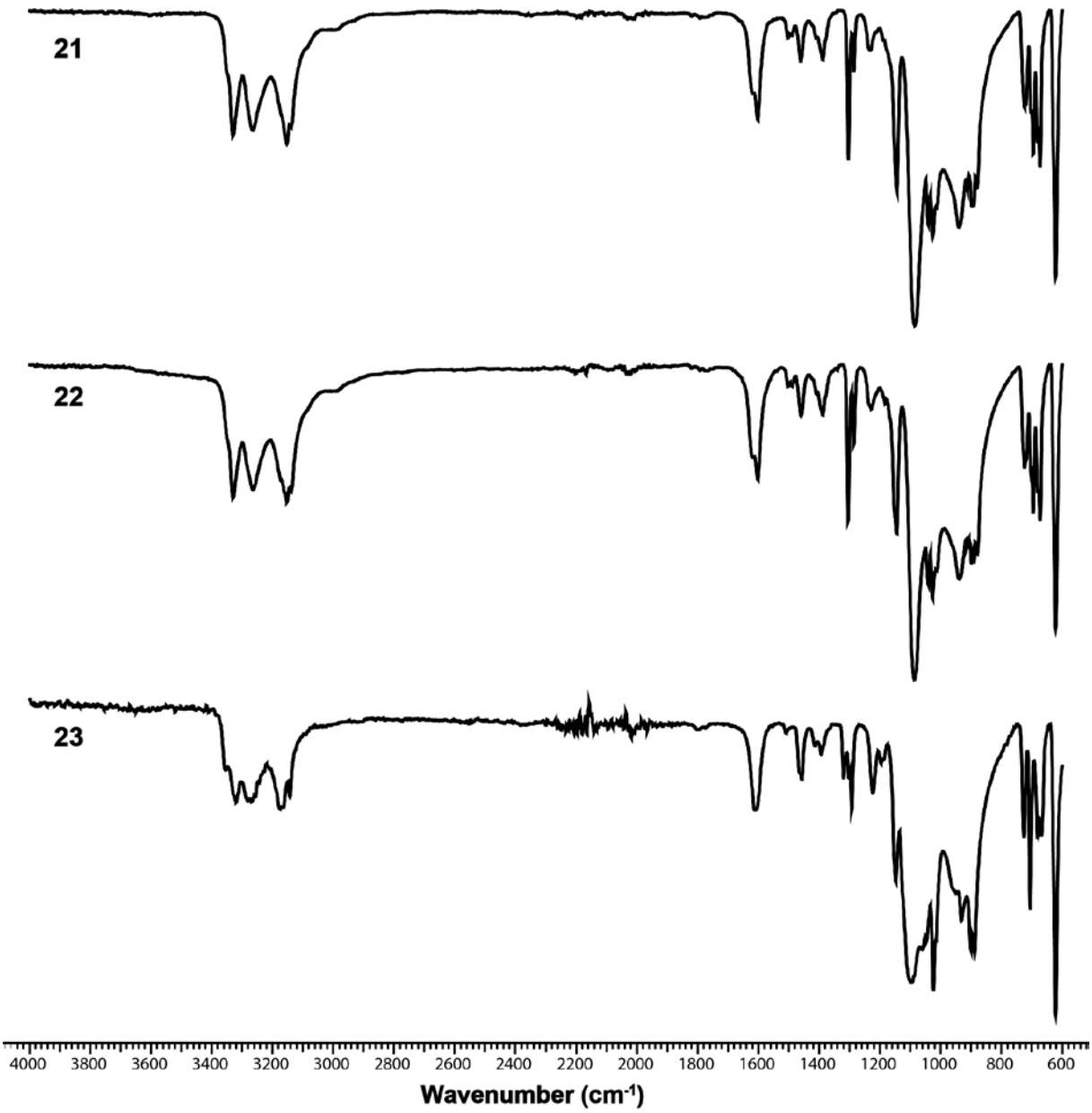

Figure S5 Infrared spectra of complexes **21**–**23**.

3. X-ray Diffraction

For all crystalline compounds, an Oxford Xcalibur3 diffractometer with a CCD area detector or Bruker D8 Venture TXS diffractometer equipped with a multilayer monochromator, a Photon 2 detector and a rotating-anode generator were employed for data collection using Mo-*K*α radiation (λ = 0.7107 Å). On the Oxford device, data collection and reduction were carried out using the CRYSALISPRO software[S1]. On the Bruker diffractometer, the data were collected with the Bruker Instrument Service v3.0.21, the data reduction was performed using the SAINT V8.18C software (Bruker AXS Inc., 2011). The structures were solved by direct methods (SIR-92[S2], SIR-97[S3] or SHELXS-97[S4]) and refined by full-matrix least-squares on *F*2 (SHELXL[S4]) and finally checked using the PLATON software[S5] integrated in the WinGX[S6] software suite. The non-hydrogen atoms were refined anisotropically and the hydrogen atoms were located and freely refined. The absorptions were corrected by a SCALE3 ABSPACK or SADABS Bruker APEX3 multiscan method[S7,8]. All DIAMOND2 plots are shown with thermal ellipsoids at the 50% probability level and hydrogen atoms are shown as small spheres of arbitrary radius. X-ray powder experiments were performed on a Gunier diffractometer (Huber G644) with Mo-*K*α1 radiation (λ = 0.7093 Å, quartz monochromator) in Lindemann capillaries (0.7 mm diameter). The angle calibration was performed with electronic grade germanium. In the 2θ range between 4 and 34° with an increment of 0.04°, 750 data points were collected with a counting rate of 10 s for each increment. The Rietveld parameters were analyzed with the program FullProf.[S9]

Table S1. Crystallographic data of **1** and **3**–**5**.

	1	**3**	**4**	**5**
Formula	CH_3N_5	$CH_4ClN_5O_4$	$C_6H_{18}Cl_2MnN_{30}O_8$	$C_6H_{18}Cl_2FeN_{30}O_8$
FW [g mol^{-1}]	85.08	185.54	764.34	765.25
Crystal system	Orthorhombic	Monoclinic	Trigonal	Trigonal
Space Group	$P2_12_12_1$	$P2_1/n$	$P\bar{3}$	$P\bar{3}$
Color / Habit	Colorless block	Colorless block	Light-rose block	Colorless block
Size [mm]	0.20 x 0.40 x 0.50	0.13 x 0.19 x 0.42	0.15 x 0.15 x 0.15	0.23 x 0.30 x 0.50
a [Å]	5.0889(3)	5.5236(4)	10.9978(13)	18.8934(4)
b [Å]	6.5662(5)	8.3025(7)	10.9978(13)	18.8934(4)
c [Å]	11.1652(8)	13.6929(11)	6.9815(11)	6.9830(2)
α [°]	90	90	90	90
β [°]	90	90.247(5)	90	90
γ [°]	90	90	120	120
V [Å^3]	373.08(4)	627.95(9)	731.3(2)	2158.70(13)
Z	4	4	1	3
$\rho_{calc.}$ [g cm^{-3}]	1.515	1.963	1.736	1.766
μ [mm^{-1}]	0.119	0.586	0.725	0.802
F(000)	176	376	387	1164
$\lambda_{MoK\alpha}$ [Å]	0.71073	0.71073	0.71073	0.71073
T [K]	173	173	143	173
θ Min–Max [°]	4.4, 26.0	4.4, 26.0	4.3, 27.5	4.3, 26.2
Dataset	−5: 6; −7: 8; −13: 13	−6: 6; −10: 10; −16: 10	−13: 14; −12: 14; −9: 8	−23: 22; −20: 23; −8: 8
Reflections collected	2753	4330	5123	16975
Independent refl.	730	1228	1085	2898
R_{int}	0.017	0.027	0.079	0.024
Observed reflections	701	1098	703	2492
Parameters	67	117	104	286
R_1 (obs)[a]	0.0208	0.0272	0.1197	0.0637
wR_2 (all data)[b]	0.0504	0.0732	0.3420	0.1923
GooF[c]	1.13	1.07	1.19	1.06
Resd. Dens. [e Å^{-3}]	−0.13, 0.12	−0.42, 0.20	−0.74, 1.07	−1.13, 1.58
Absorption correction	multi-scan	multi-scan	multi-scan	multi-scan
CCDC	1834855	1834849	—	1834847

a) $R_1 = \Sigma||F_0|- |F_c||/ \Sigma|F_0|$; b) $wR_2 = [\Sigma[w(F_0^2-F_c^2)^2]/\Sigma[w(F_0)^2]]^{1/2}$; $w = [\sigma c^2(F_0^2)+(xP)^2+yP]^{-1}$ and $P=(F_0^2+2F_c^2)/3$; c) GooF = $\{\Sigma[w(F_o^2-F_c^2)^2]/(n-p)\}^{1/2}$ (n = number of reflections; p = total number of parameters).

Table S2. Crystallographic data of **6**–**9**.

	6	**7**	**8**	**9**
Formula	$C_6H_{18}Cl_2CuN_{30}O_8$	$C_6H_{18}Cl_2N_{30}O_8Zn$	$C_2H_6Cl_2CuN_{10}$	$C_3H_9CuN_{17}O_6$
FW [g mol^{-1}]	772.94	774.77	304.61	442.81
Crystal system	Trigonal	Trigonal	Monoclinic	Monoclinic
Space Group	*P*−3	*P*−3	$P2_1/n$	*Cc*
Color / Habit	Blue block	Colorless block	Green block	Blue block
Size [mm]	0.14 x 0.20 x 0.28	0.10 x 0.32 x 0.38	0.09 x 0.13 x 0.20	0.11 x 0.12 x 0.34
a [Å]	21.8207(4)	18.908(5)	7.4976(2)	15.301(5)
b [Å]	21.8207(4)	18.908(5)	12.2023(5)	6.684(5)
c [Å]	6.9043(5)	6.992(5)	10.3115(4)	15.203(5)
α [°]	90	90	90	90
β [°]	90	90	91.719	106.027(5)
γ [°]	120	120	90	90
V [Å^3]	2847.00(19)	2165(2)	942.95(6)	1494.4(13)
Z	4	3	4	4
$\rho_{calc.}$ [g cm^{-3}]	1.803	1.783	2.146	1.968
μ [mm^{-1}]	1.049	1.129	2.867	1.539
F(000)	1564	1176	604	892
$\lambda_{MoK\alpha}$ [Å]	0.71073	0.71073	0.71073	0.71073
T [K]	173	173	173	173
θ Min–Max [°]	4.3, 27.0	4.3, 26.5	4.3, 26.0	4.1, 28.0
Dataset	−25: 27; −27: 27; −8: 8	−15: 23; −23: 22; −8: 8	−9: 9; −14:15; −12: 12	−20: 19; −7: 8; −16: 20
Reflections collected	15966	17769	6823	6665
Independent refl.	4111	2987	1846	2808
R_{int}	0.035	0.026	0.027	0.041
Observed reflections	2713	2571	1625	2567
Parameters	347	262	160	269
R_1 (obs)[a]	0.0628	0.0661	0.0224	0.0328
wR_2 (all data)[b]	0.1925	0.2024	0.0564	0.0575
GooF[c]	1.04	1.04	1.09	1.03
Resd. Dens. [e Å^{-3}]	−1.01, 1.47	−0.66, 3.07	−0.33, 0.34	−0.32, 0.31
Absorption correction	multi-scan	multi-scan	multi-scan	multi-scan
CCDC	1834859	1834851	1834845	1834844

a) $R_1 = \Sigma||F_0|- |F_c||/ \Sigma|F_0|$; b) $wR_2 = [\Sigma[w(F_0^2-F_c^2)^2]/\Sigma[w(F_0)^2]]^{1/2}$; $w = [\sigma c^2(F_0^2)+(xP)^2+yP]^{-1}$ and $P=(F_0^2+2F_c^2)/3$; c) GooF = $\{\Sigma[w(F_o^2-F_c^2)^2]/(n-p)\}^{1/2}$ (n = number of reflections; p = total number of parameters).

Table S3. Crystallographic data of **10** and **12**–**14**.

	10	**12**	**13**	**14**
Formula	$C_6H_{18}Cl_2CuN_{30}O_6$	$C_6H_{18}N_{32}O_6Zn$	$C_{14}H_{22}MnN_{16}O_{22}$	$C_{14}H_{22}MnN_{16}O_{24}$
FW [g mol^{-1}]	740.94	699.89	821.41	853.41
Crystal system	Monoclinic	Monoclinic	Monoclinic	Monoclinic
Space Group	$P2_1/c$	$P2_1/n$	$P2_1/c$	$P2_1/c$
Color / Habit	Blue block	Colorless block	Yellow block	Colorless block
Size [mm]	0.11 x 0.23 x 0.32	0.20 x 0.30 x 0.40	0.20 x 0.40 x 0.42	0.16 x 0.22 x 0.28
a [Å]	9.6517(3)	9.4477(10)	14.7040(6)	14.8973(9)
b [Å]	7.8880(3)	7.9116(9)	5.0490(2)	5.0185(2)
c [Å]	17.1904(5)	17.279(2)	20.4680(9)	20.4159(10)
α [°]	90	90	90	90
β [°]	93.923(2)	90.610(11)	103.858(4)	103.628(5)
γ [°]	90	90	90	90
V [Å^3]	1305.68(7)	1291.5(3)	1475.32(11)	1483.36(13)
Z	2	2	2	2
$\rho_{calc.}$ [g cm^{-3}]	1.885	1.800	1.849	1.911
μ [mm^{-1}]	1.133	1.047	0.573	0.578
F(000)	750	712	838	870
$\lambda_{MoK\alpha}$ [Å]	0.71073	0.71073	0.71069	0.71073
T [K]	173	173	143	143
θ Min–Max [°]	4.2, 26.0	4.2, 26.0	4.2, 26.0	4.2, 26.5
Dataset	−11: 11; −9: 6; −21: 21	−11: 11; −9: 9; −21: 20	−18: 18; −4:6; −25: 24	−18: 18; −6:6; −21: 25
Reflections collected	9613	9361	10483	11409
Independent refl.	2549	2524	2885	3029
R_{int}	0.033	0.080	0.028	0.052
Observed reflections	2372	1856	2540	2410
Parameters	229	229	274	294
R_1 (obs)[a]	0.0647	0.0667	0.0278	0.0377
wR_2 (all data)[b]	0.1425	0.1725	0.0722	0.0794
GooF[c]	1.35	1.09	1.05	1.05
Resd. Dens. [e Å^{-3}]	−0.89, 0.81	−0.93, 1.12	−0.22, 0.30	−0.30, 0.35
Absorption correction	multi-scan	multi-scan	multi-scan	multi-scan
CCDC	1834853	1834852	1834858	1834857

a) $R_1 = \Sigma||F_0|- |F_c||/ \Sigma|F_0|$; b) $wR_2 = [\Sigma[w(F_0^2-F_c^2)^2]/\Sigma[w(F_0)^2]]^{1/2}$; $w = [\sigma c^2(F_0^2)+(xP)^2+yP]^{-1}$ and $P=(F_0^2+2F_c^2)/3$; c) GooF = $\{\Sigma[w(F_o^2-F_c^2)^2]/(n-p)\}^{1/2}$ (n = number of reflections; p = total number of parameters).

Table S4. Crystallographic data of **15**–**18**.

	15	**16**	**17**	**18**
Formula	$C_4H_{16}MnN_{20}Cl_2O_{10}$	$C_2H_6Cl_2CuN_{10}$	$C_2H_6CuN_{12}O_6$	$C_4H_{16}Cl_2CuN_{20}O_{10}$
FW [g mol^{-1}]	630.21	304.61	357.73	638.82
Crystal system	Triclinic	Monoclinic	Monoclinic	Tetragonal
Space Group	*P*−1	$P2_1/c$	$P2_1/n$	$P4_2/n$
Color / Habit	Colorless block	Green block	Blue plate	Blue block
Size [mm]	0.22 x 0.71 x 0.96	0.12 x 0.17 x 0.34	0.12 x 0.36 x 0.44	0.10 x 0.15 x 0.40
a [Å]	7.8980(5)	6.8468(5)	7.9953(8)	10.3883(3)
b [Å]	9.6180(6)	3.6679(2)	8.9746(8)	10.3883(3)
c [Å]	15.7710(7)	18.5122(12)	8.0033(9)	10.0967(8)
α [°]	78.554(4)	90	90	90
β [°]	76.267(4)	91.579(6)	107.469(12)	90
γ [°]	73.230(5)	90	90	90
V [Å^3]	1103.34(11)	464.73(5)	547.79(10)	1089.60(11)
Z	2	2	2	2
$\rho_{calc.}$ [g cm^{-3}]	1.897	2.177	2.169	1.947
μ [mm^{-1}]	0.933	2.909	2.058	1.342
F(000)	638	302	358	646
$\lambda_{MoK\alpha}$ [Å]	0.710769	0.71073	0.71073	0.71073
T [K]	173	173	173	173
θ Min–Max [°]	4.3, 26.0	4.4, 26.0	4.3, 26.5	4.4, 26.0
Dataset	−9: 9; −11: 11; −19: 17	−8: 8; −4: 4; −22: 22	−9: 10; −7: 11; −10: 10	−12: 11; −12:8; −12: 12
Reflections collected	8333	2907	4198	8313
Independent refl.	4311	920	1121	1067
R_{int}	0.018	0.031	0.027	0.053
Observed reflections	3820	831	1024	879
Parameters	386	82	109	113
R_1 (obs)[a]	0.0378	0.0246	0.0229	0.0389
wR_2 (all data)[b]	0.0974	0.0596	0.0635	0.1049
GooF[c]	1.04	1.07	1.05	1.06
Resd. Dens. [e Å^{-3}]	−0.95, 1.39	−0.44, 0.40	−0.34, 0.30	−0.64, 0.74
Absorption correction	multi-scan	multi-scan	multi-scan	multi-scan
CCDC	1834854	1834842	1834843	1834841

a) $R_1 = \Sigma||F_0|- |F_c||/ \Sigma|F_0|$; b) $wR_2 = [\Sigma[w(F_0^2-F_c^2)^2]/\Sigma[w(F_0)^2]]^{1/2}$; $w = [\sigma c^2(F_0^2)+(xP)^2+yP]^{-1}$ and $P=(F_0^2+2F_c^2)/3$; c) GooF = $\{\Sigma[w(F_o^2-F_c^2)^2]/(n-p)\}^{1/2}$ (n = number of reflections; p = total number of parameters).

Table S5. Crystallographic data of **19**–**23**.

	19	**20**	**21**	**22**	**23**
Formula	$C_5H_{17}Cl_2FeN_{25}O_9$	$C_5H_{17}Cl_2N_{25}O_9Zn$	$C_8H_{24}Cl_2FeN_{40}O_8$	$C_8H_{24}Cl_2N_{40}O_8Zn$	$C_8H_{24}Cl_2CuN_{40}O_8$
FW [g mol^{-1}]	698.19	707.71	935.42	944.94	943.11
Crystal system	Triclinic	Triclinic	Triclinic	Triclinic	Triclinic
Space Group	*P*−1	*P*−1	*P*−1	*P*−1	*P*−1
Color / Habit	Colorless block	Colorless block	Colorless block	Colorless plate	Blue block
Size [mm]	0.23 x 0.35 x 0.64	0.17 x 0.31 x 0.51	0.26 x 0.32 x 0.42	0.07 x 0.17 x 0.27	0.10 x 0.10 x 0.40
a [Å]	9.4770(6)	9.4977(6)	8.5130(3)	8.5016(2)	10.3015(7)
b [Å]	9.9109(6)	9.9017(5)	10.8300(5)	10.8035(3)	10.8660(7)
c [Å]	15.4054(8)	15.3665(8)	19.3050(8)	19.2662(6)	16.4236(11)
α [°]	75.695(5)	75.918(5)	79.072(4)	79.175(3)	80.433(6)
β [°]	89.058(5)	89.336(5)	86.098(3)	86.100(2)	73.574(6)
γ [°]	63.694(6)	63.594(6)	86.476(3)	86.315(2)	80.646(5)
V [Å^3]	1249.66(15)	1247.54(14)	1741.78(13)	1731.63(8)	1725.8(2)
Z	2	2	2	2	2
$\rho_{calc.}$ [g cm^{-3}]	1.855	1.884	1.784	1.812	1.815
μ [mm^{-1}]	0.912	1.293	0.689	0.966	0.891
F(000)	708	716	952	960	958
$\lambda_{MoK\alpha}$ [Å]	0.71073	0.71073	0.71073	0.71073	0.71073
T [K]	173	173	173	173	143
θ Min–Max [°]	4.1, 26.0	4.3, 26.0	4.3, 26.0	4.3, 26.0	4.1, 26.0
Dataset	−11: 10; −12:11; −17: 19	−11: 8; −12: 12; −18: 18	−9: 10; −13: 13; −23: 23	−10: 10; −13: 13; −23: 22	−10: 12; −13:13; −20: 20
Reflections collected	10053	9906	13629	14327	13551
Independent refl.	4884	4875	6835	6784	6759
R_{int}	0.023	0.028	0.023	0.033	0.039
Observed reflections	4136	4264	5770	5317	5061
Parameters	484	475	628	628	599
R_1 (obs)[a]	0.0473	0.0474	0.0317	0.0369	0.0403
wR_2 (all data)[b]	0.1369	0.1348	0.0821	0.0874	0.0951
GooF[c]	1.04	1.05	1.03	1.03	1.03
Resd. Dens. [e Å^{-3}]	−1.33, 2.49	−1.18, 2.75	−0.40, 0.45	−0.40, 0.39	−0.46, 0.36
Absorption correction	multi-scan	multi-scan	multi-scan	multi-scan	multi-scan
CCDC	1834856	1834846	1834848	1834850	1838980

a) $R_1 = \Sigma||F_0|- |F_c||/ \Sigma|F_0|$; b) $wR_2 = [\Sigma[w(F_0^2-F_c^2)^2]/\Sigma[w(F_0)^2]]^{1/2}$; $w = [\sigma c^2(F_0^2)+(xP)^2+yP]^{-1}$ and $P=(F_0^2+2F_c^2)/3$; c) GooF = $\{\Sigma[w(F_o^2-F_c^2)^2]/(n-p)\}^{1/2}$ (n = number of reflections; p = total number of parameters).

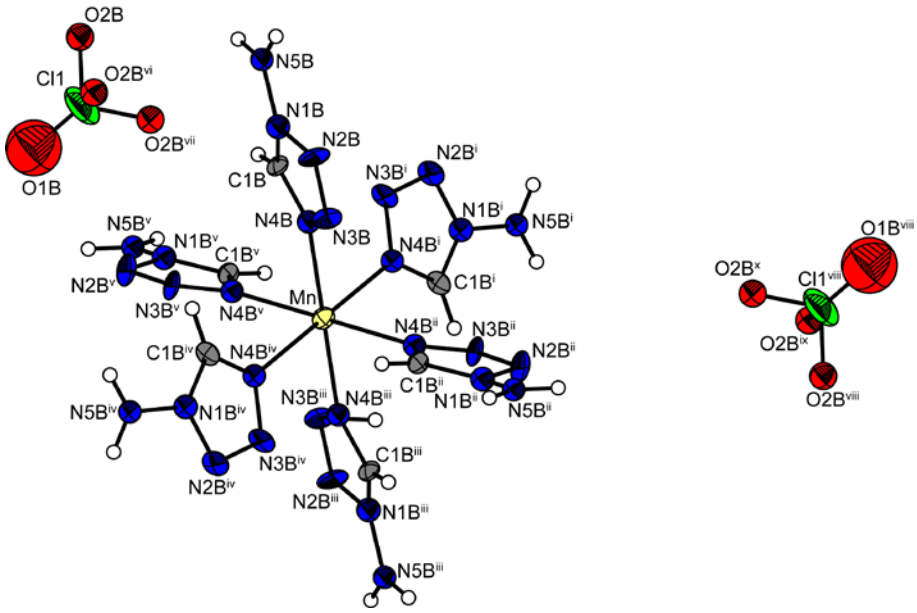

Figure S6 Molecular unit of $[Mn(1\text{-}AT)_6](ClO_4)_2$ (**4**). Selected bond length (Å): Mn–N4B 2.28(2); selected bond angles (°): N4B–Mn–N4B^{iv} 89.9(8), N4B–Mn–N4B^{i} 90.2(8i), and N4B–Mn–N4B^{iii} 180.00. Symmetry codes: (i) 1+y, 1−x+y, 2−z; (ii) x−y, −1+x, 2−z; (iii) 2–x, −y, 2−z; (iv) 1−y, −1+x−y, z; (v) 2–x+y, 1−x, z; (vi) 2−x, −y, 1−z; (vii) 2+y, 1−x+y, 1−z; (viii) 1+x−y, x, 1−z; (ix) 1−x+y, −x, z; (x) −y, −1+x−y, z.

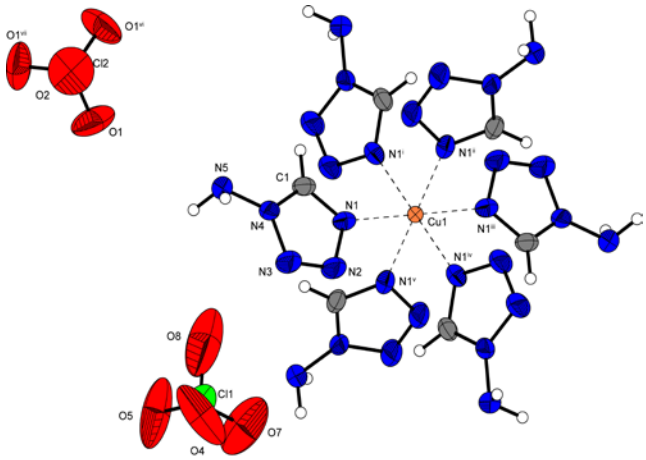

Figure S7 Molecular unit of $[Cu(1\text{-}AT)_6](ClO_4)_2$ (**6**). Selected bond length (Å): Cu1–N1 2.127(4); selected bond angles (°): N1–Cu1–N1^{iii} 91.79(17), N1–Cu1–N1^{vi} 88.21(17), N1^{iii}–Cu1–N1^{iv} 91.8(2), N1^{iii}–Cu1–N1^{vii} 88.2(2). Symmetry codes: (i) −x, −y, −z; (ii) x−y, x, −z; (iii) −x+y, −x, z; (iv) −y, x−y, z; (v) y, −x+y, −z; (vi) −x, 1−y, −z; (vii) 1−x+y, 1−x, z.

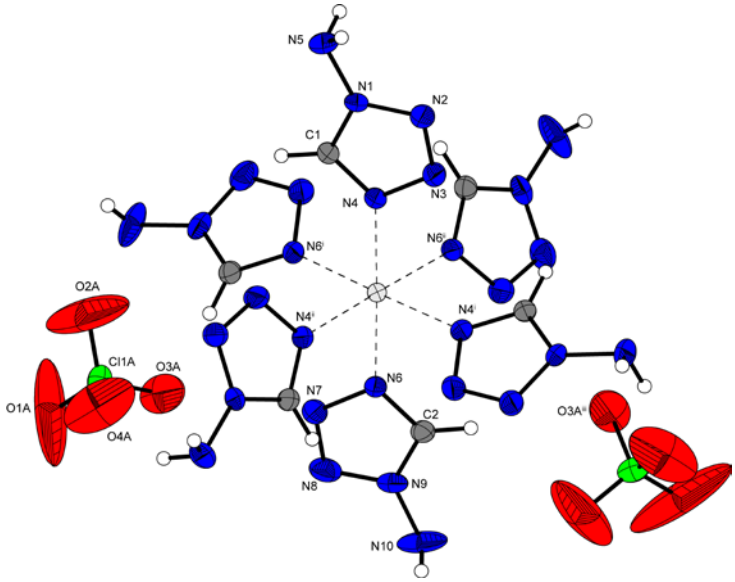

Figure S8 Molecular unit of $[Zn(1\text{-}AT)_6](ClO_4)_2$ (**7**). Selected bond lengths (Å): Zn1–N4 2.167(4), Zn1–N6 2.167(4), Zn2–N14 2.167(4); selected bond angles (°): N14–Zn2–$N14^{vii}$ 88.78(13), $N14^{iii}$–Zn2–$N14^{iv}$ 91.23(18), N4–Zn1–N6 178.62(15), N4–Zn1–$N4^{i}$ 91.07(16), N4–Zn1–$N6^{i}$ 89.98(16), N4–Zn1–$N6^{ii}$ 88.01(14), N6–Zn1–$N6^{i}$ 90.96(16). Symmetry codes: (i) 1−y, x−y, z; (ii) 1−x+y, 1−x, z; (iii) −x, −y, −z.

The unmanageable, extremely sensitive copper(II) chlorate coordination compounds **10** and **11** crystallize both in the form of blue blocks in the monoclinic space group $P2_1/n$ and the triclinic space group $P\bar{1}$, respectively. The calculated densities vary only slightly, with 1.885 g cm^{-3} (173 K) (**10**) and 1.959 g cm^{-3} (143 K) (**11**) from each other. Both complexes consist of closed octahedral coordination spheres with six and four coordinated 1-AT ligands. While in compound **10** the chlorate counter-anions are non-coordinating (Figure S9), they act as chlorato ligands in complex **11**. Similar to complex **4**, a high degree of disorder can be observed for the coordinating heterocycles and anions in the X-ray structure of the tetrakis(1-amino-5*H*-tetrazolyl) compound **11**, which unfortunately only allows an isotropic refinement of its data set (Figure S10).

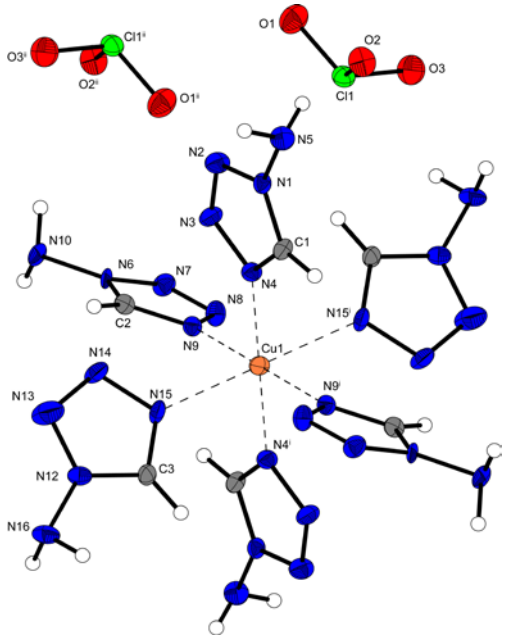

Figure S9 Molecular unit of $[Cu(1\text{-}AT)_6](ClO_3)_2$ (**10**). Selected bond lengths (Å): Cu1–N4 2.054(4), Cu1–N9 2.012(4), Cu1–N15 2.403(5); selected bond angles (°): N4–Cu1–N9 89.46(16), N4–Cu1–N15 90.15(16), N4–Cu1–N4^{i} 180.00. Symmetry codes: (i) 1−x, −y, 2−z; (ii) 2−x, 1−y, 2−z.

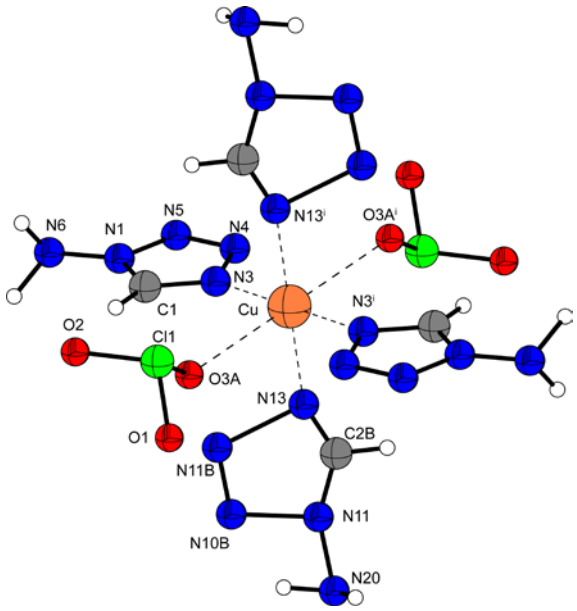

Figure S10 Isotropic illustration of the molecular unit of $[Cu(ClO_3)_2(1\text{-}AT)_4]$ (**11**).

$[Zn(1\text{-}AT)_6](NO_3)_2$ (**12**) crystallizes in the form of colorless blocks in the monoclinic space group $P2_1/n$ with two formula units per unit cell and a calculated density of 1.800 g cm^{-3} at

173 K. The metal(II) center is coordinated by six tetrazole ligands with Zn–N bonds in the range of 2.165(4)-2.175(4) Å and therefore forms an almost perfect octahedral structure with bond angles close to 90° (Figure S12).

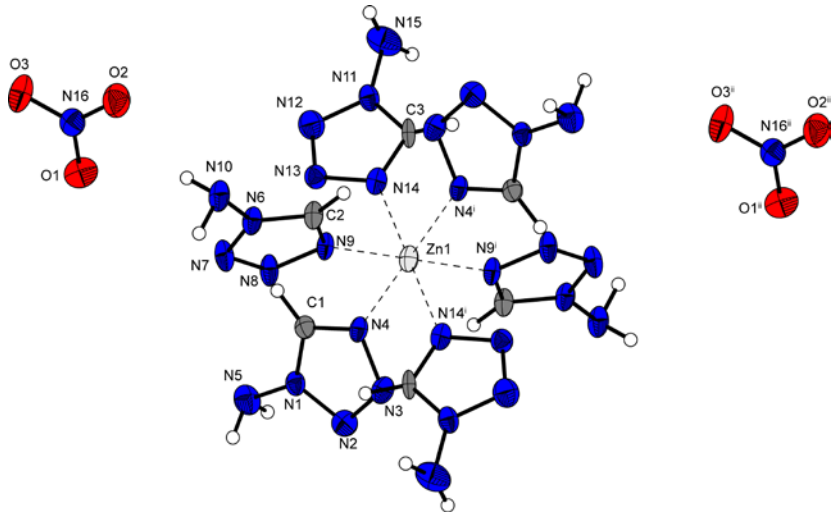

Figure S11 Molecular unit of $[Zn(1\text{-}AT)_6](NO_3)_2$ (**12**). Selected bond lengths (Å): Zn1–N4 2.165(4), Zn1–N9 2.171(4), Zn1–N14 2.175(4); selected bond angles (°): N4–Zn1–N9 90.42(14), N4–Zn1–N14 90.24(14), N9–Zn1–N14 90.29(14). Symmetry codes: (i) 2−x, −y, −z; (ii) 1+x, −2+y, z.

$[Mn(H_2O)_6](HTNR)_2 \cdot 2$ 2-AT (**13**) as well as $[Mn(H_2O)_6](H_2TNPG)_2 \cdot 2$ 2-AT (**14**) both did not form coordination compounds with 1-AT but crystallized as hexaaqua complexes with either $HTNR^-$ or H_2TNPG^- as counter-anions and cocrystallizing 1-AT molecules. Both compounds crystallize in the monoclinic space group $P2_1/c$ with two formula units per unit cell and calculated densities of 1.849 g cm^{-3} and 1.911 g cm^{-3} at 143 K, respectively. The Mn–O bonds differ only slightly in both compounds (**13**: 2.1355(12)-2.2037(13) Å; **14**: 2.140(2)-2.1874(18) Å) forming octahedral structures with negligible deformations (Figure S13 and S14).

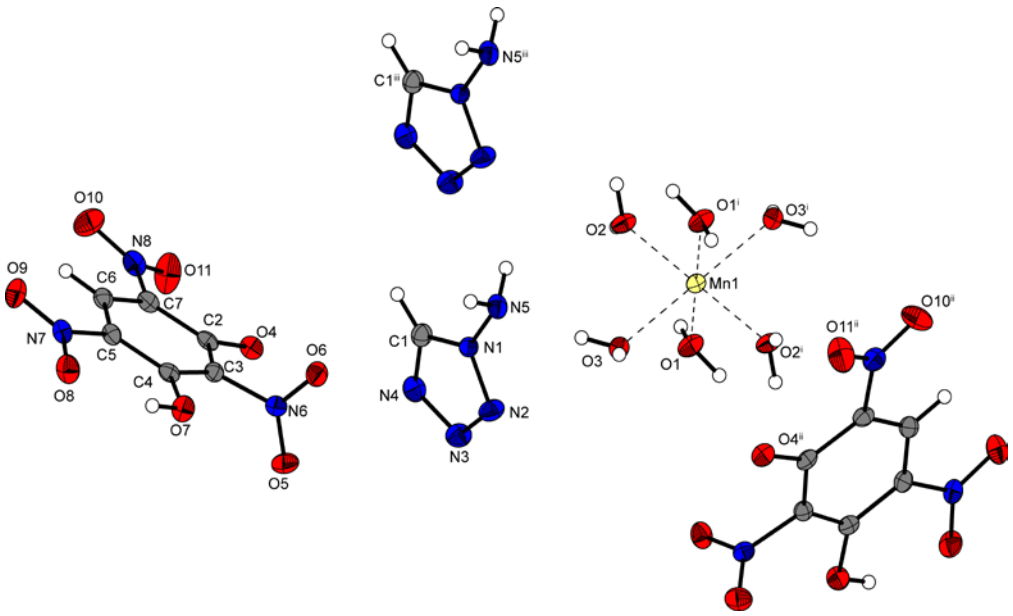

Figure S12 Molecular unit of $[Mn(H_2O)_6](HTNR)_2 \cdot 2$ 2-AT (**13**). Selected bond length (Å): Mn1–O1 2.1925(14), Mn1–O2 2.1355(12), Mn1–O3 2.2037(13); selected bond angles (°): O1–Mn1–O2 95.90(5), O1–Mn1–O3 92.27(5), O2–Mn1–O3 89.57(5). Symmetry codes: (i) 1−x, −y, −z; (ii) 1−x, 0.5+y, 0.5−z; (iii) x, −1+y, z.

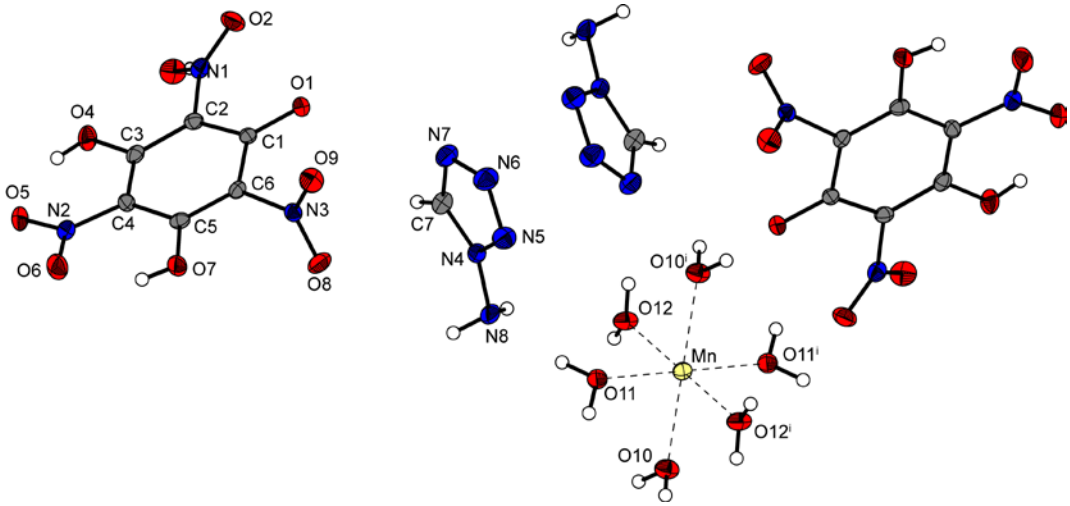

Figure S13 Molecular unit of $[Mn(H_2O)_6](H_2TNPG)_2 \cdot 2$ 2-AT (**14**). Selected bond lengths (Å): Mn–O10 2.1861(18), Mn–O11 2.1874(18), Mn–O12 2.140(2); selected bond angles (°): O10–Mn–O11 88.78(7), O10–Mn–O12 83.00(7). Symmetry code: (i) 1−x, 1−y, −z.

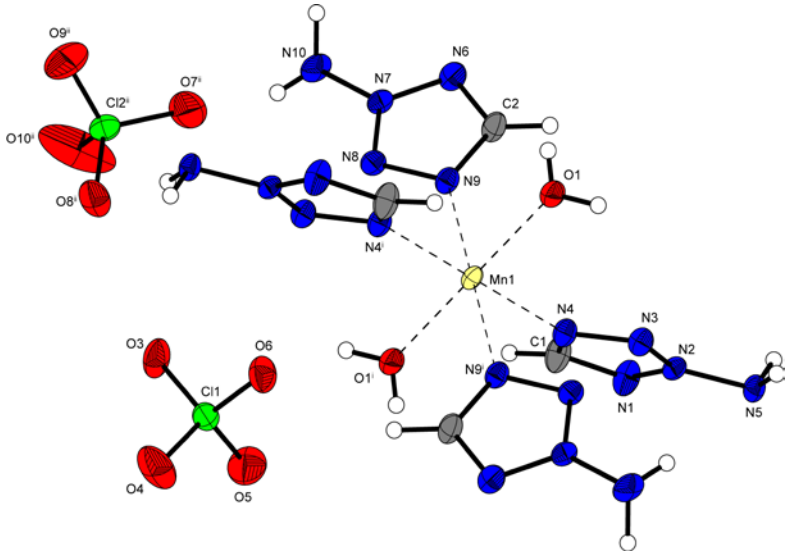

Figure S14 Molecular unit of $[Mn(H_2O)_2(2\text{-AT})_4](ClO_4)_2$ (**15**). Selected bond lengths (Å): Mn1–O1 2.142(2), Mn1–N4 2.245(2), Mn1–N9 2.268(2); selected bond angles (°): O1–Mn1–N4 85.86(8), O1–Mn1–N9 92.28(7). Symmetry codes: (i) −x, 1−y, 1−z; (ii) −1+x, y, z.

The exceptionality of the structure of **17** becomes clear when viewing along the *a*-axis (Figure S15). Brought about by the previously mentioned bridging 2-AT, a grid pattern, consisting of crosswise arranged one dimensional chains of **17**, can be observed. The distance between the copper(II) centers of adjacent chains of the same alignment is 8.975 Å, a value that resembles the lattice parameter b of the unit cell. The metal(II) centers in between the chains themselves are 6.521 Å apart from each other. The complete topology is revealed regarding the compound's crystal structure along the *b*-axis (Figure S16): The two-dimensional grid patterns that have been mentioned beforehand form a layer structure whose components are held together by several hydrogen bonds (Table S7). The respective layers are aligned parallel to the plane built up by the unit cell's b-axis and the diagonal through the a-c-plane.

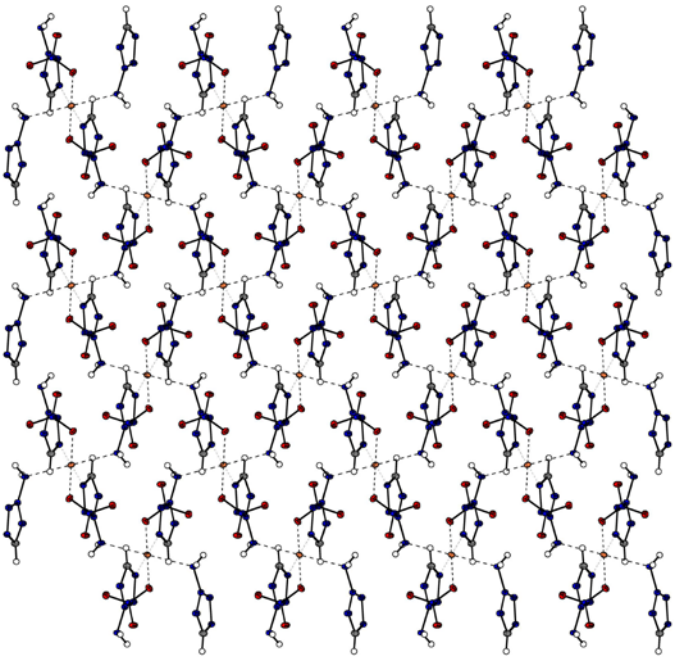

Figure S15 Grid pattern of **17** by viewing along the *a*-axis.

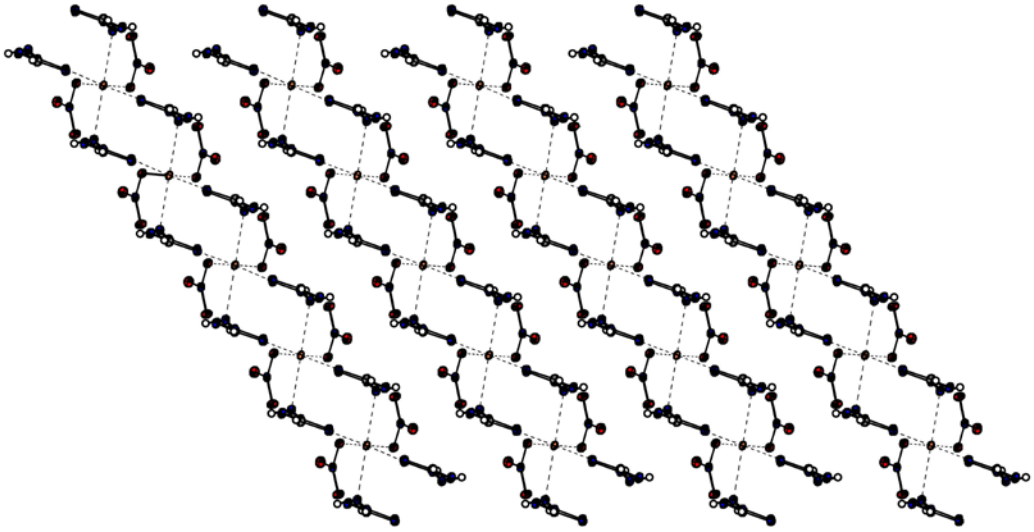

Figure S16 Structure of **17** with the direction of view along the *b*-axis.

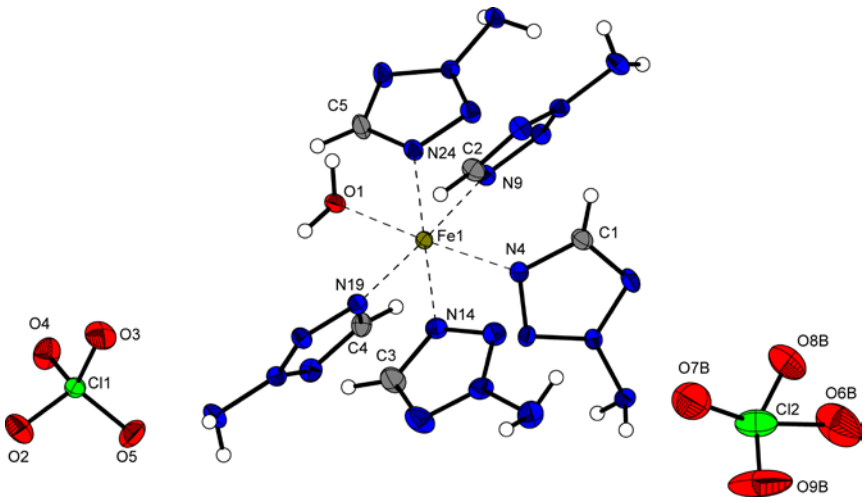

Figure S17 Molecular unit of $[Fe(H_2O)(2\text{-}AT)_5](ClO_4)_2$ (**19**). Selected bond lengths (Å): Fe1–O1 2.070(3), Fe1–N4 2.185(3), Fe1–N9 2.212(3), Fe1–N14 2.175(3), Fe1–N19 2.192(3), Fe1–N24 2.181(3); selected bond angles (°): O1–Fe1–N4 176.31(10), N9–Fe1–N19 176.18(12), N14–Fe1–N24 178.61(11), O1–Fe1–N9 86.02(11), O1–Fe1–N14 92.34(11), O1–Fe1–N24 87.60(11), N4–Fe1–N9 92.63(11), N4–Fe1–N14 91.03(11), N9–Fe1–N14 87.54(10), N9–Fe1–N24 91.06(10), N14–Fe1–N19 91.21(10).

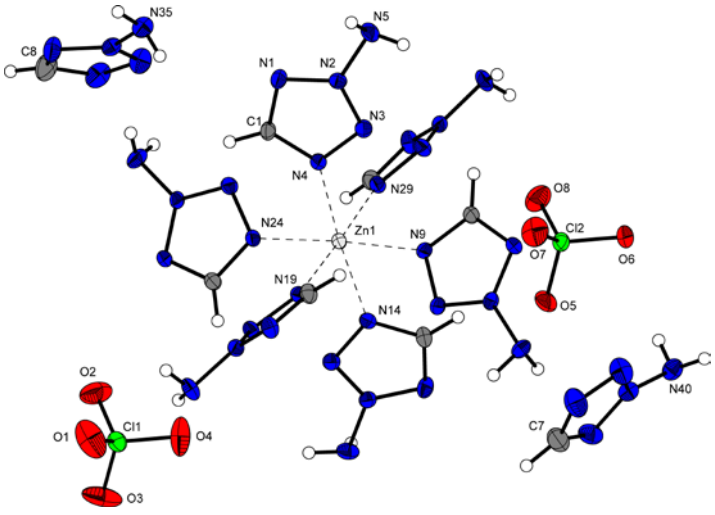

Figure S18 Molecular unit of $[Zn(2\text{-}AT)_6](ClO_4)_2 \cdot 2$ 2-AT (**22**). Selected bond lengths (Å): Zn1–N4 2.159(2), Zn1–N9 2.200(2), Zn1–N14 2.210(2), Zn1–N19 2.1303(18), Zn1–N24 2.206(2), Zn1–N29 2.1218(18); selected bond angles (°): N4–Zn1–N14 175.56(8), N9–Zn1–N24 176.19(8), N19–Zn1–N29 177.56(8), N4–Zn1–N9 89.61(8), N4–Zn1–N19 88.35(7), N4–

Zn1–N24 93.16(8), N4–Zn1–N29 89.30(7), N9–Zn1–N14 86.38(7), N9–Zn1–N19 87.49(7), N9–Zn1–N29 93.17(7), N14–Zn1–N19 93.36(7), N14–Zn1–N24 90.93(7), N14–Zn1–N29 89.03(7), N19–Zn1–N24 89.98(7), N24–Zn1–N29 89.49(7).

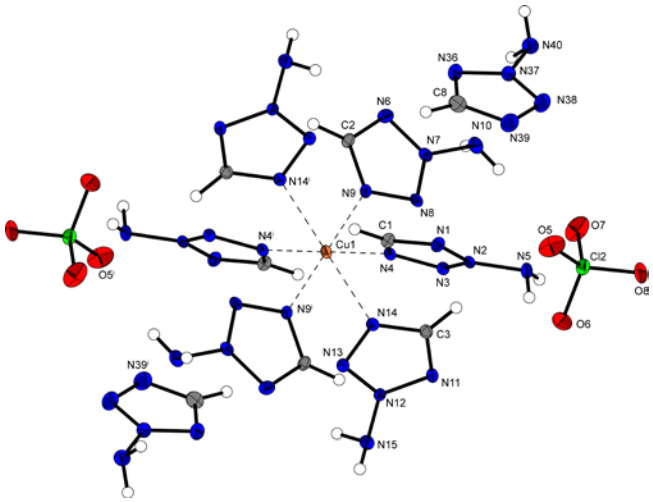

Figure S19 Molecular unit of $[Cu(2\text{-}AT)_6](ClO_4)_2 \cdot 2$ 2-AT (**23**). Selected bond lengths (Å): Cu1–N4 2.059(2), Cu1–N9 2.001(2), Cu1–N14 2.430(2); selected bond angles (°): N4–Cu1–N9 90.75(9), N4–Cu1–N14 90.65(8), N4–Cu1–$N4^{i}$ 180.00. Symmetry code: (i) −x, 2−y, −z.

Table S6. Selected hydrogen bonds in $[Fe(1\text{-}AT)_6](ClO_4)_2$ (**5**).

D–H··A	d(D–H) (Å)	d(H··A) (Å)	d(D··A) (Å)	<D–H··A (°)
N5–H5A··N15	0.80(3)	2.43(3)	3.143(5)	151(4)
N5–H5B··O3B	0.80(3)	2.42(5)	3.090(17)	142(4)
N10–H10A··O2B	0.80(7)	2.39(6)	3.107(14)	151(6)
N10–H10B··O3B	0.79(3)	2.36(5)	3.086(14)	153(6)
N15–H15A··N7	0.84(5)	2.48(5)	3.236(5)	151(5)
C1–H1··O1B	0.88(6)	2.60(6)	3.42(2)	156(4)

Table S7. Selected hydrogen bonds in $[Cu(NO_3)_2(\mu\text{-}2\text{-}AT)_4]$ (**17**).

D–H··A	d(D–H) (Å)	d(H··A) (Å)	d(D··A) (Å)	<D–H··A (°)

N5–H5A··N15	0.80(3)	2.43(3)	3.143(5)	151(4)
N5–H5B··O3B	0.80(3)	2.42(5)	3.090(17)	142(4)
N10–H10A··O2B	0.80(7)	2.39(6)	3.107(14)	151(6)
N10–H10B··O3B	0.79(3)	2.36(5)	3.086(14)	153(6)
N15–H15A··N7	0.84(5)	2.48(5)	3.236(5)	151(5)
C1–H1··O1B	0.88(6)	2.60(6)	3.42(2)	156(4)

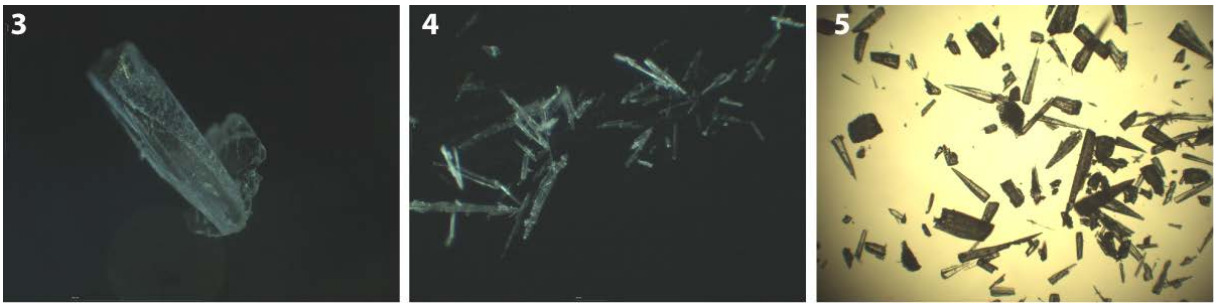

Figure S20 Microscope images of **3**–**5** (fourfold magnitude).

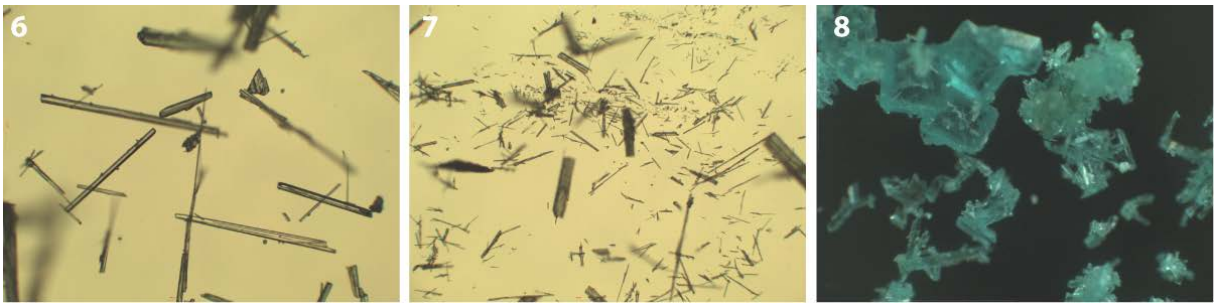

Figure S21 Microscope images of **6**–**8** (**6** and **7**: tenfold magnitude; **8**: fourfold magnitude).

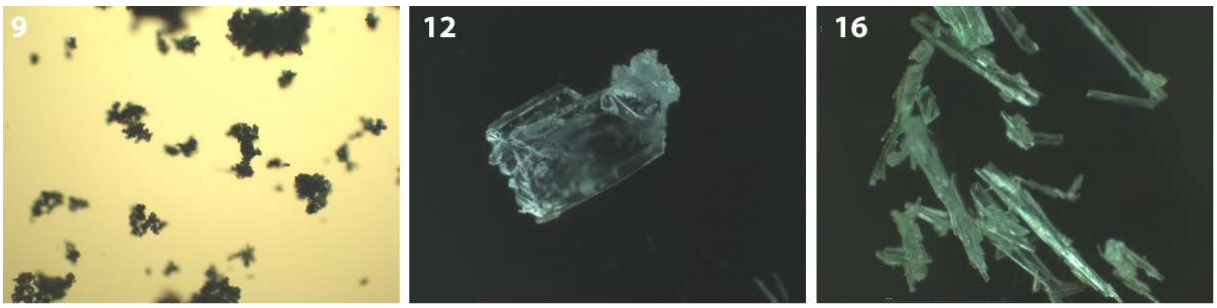

Figure S22 Microscope images of **9**, **12**, and **16** (**9**: tenfold magnitude; **12** and **16**: fourfold magnitude).

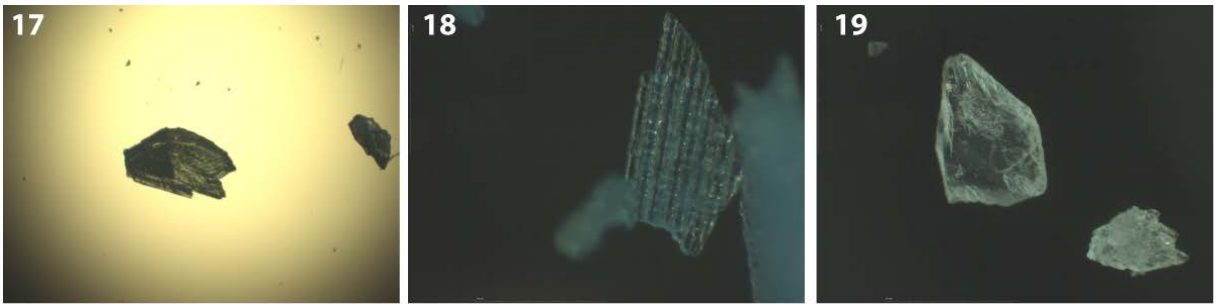

Figure S23 Microscope images of **17**–**19** (fourfold magnitude).

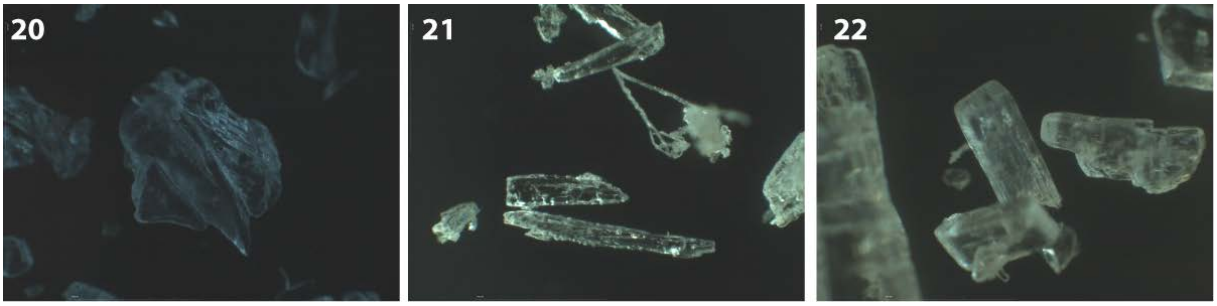

Figure S24 Microscope images of **20**–**22** (fourfold magnitude).

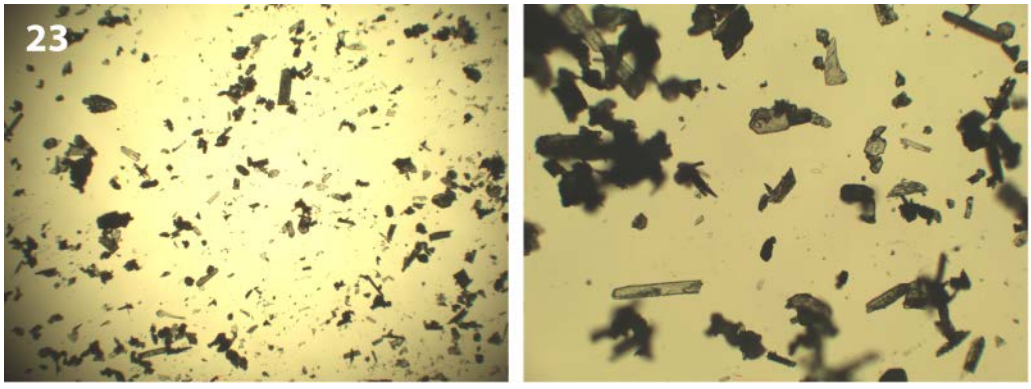

Figure S25 Microscope images of **23** (left: fourfold magnitude; right: tenfold magnitude).

4. TGA plots of 1 and 2

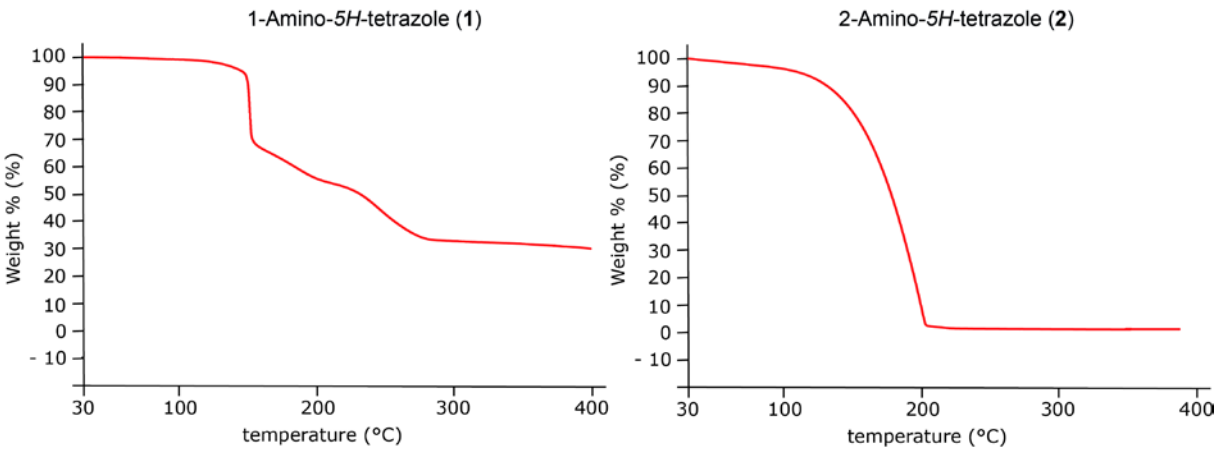

Figure S26 TGA plots of **1** and **2**.

5. DTA plots of 1–3, 8, 9, 12 and 16–23

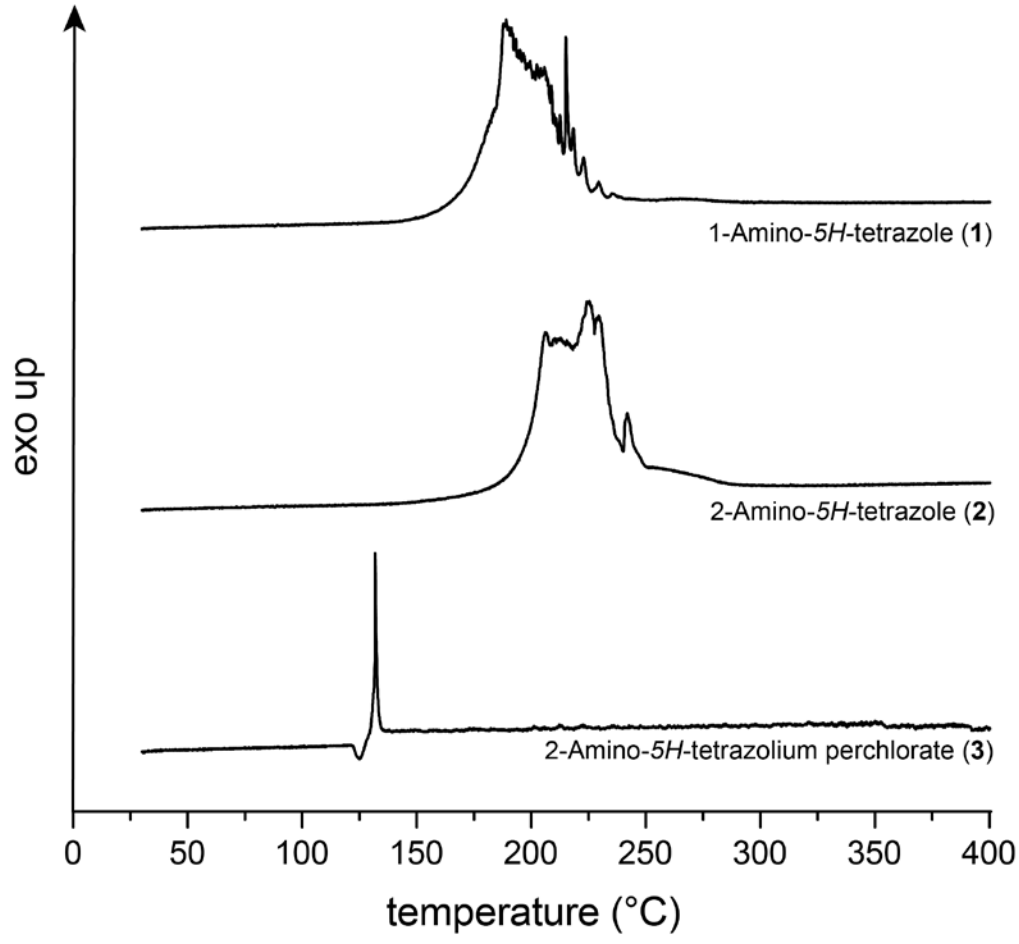

Figure S27 DTA plots of **1–3**.

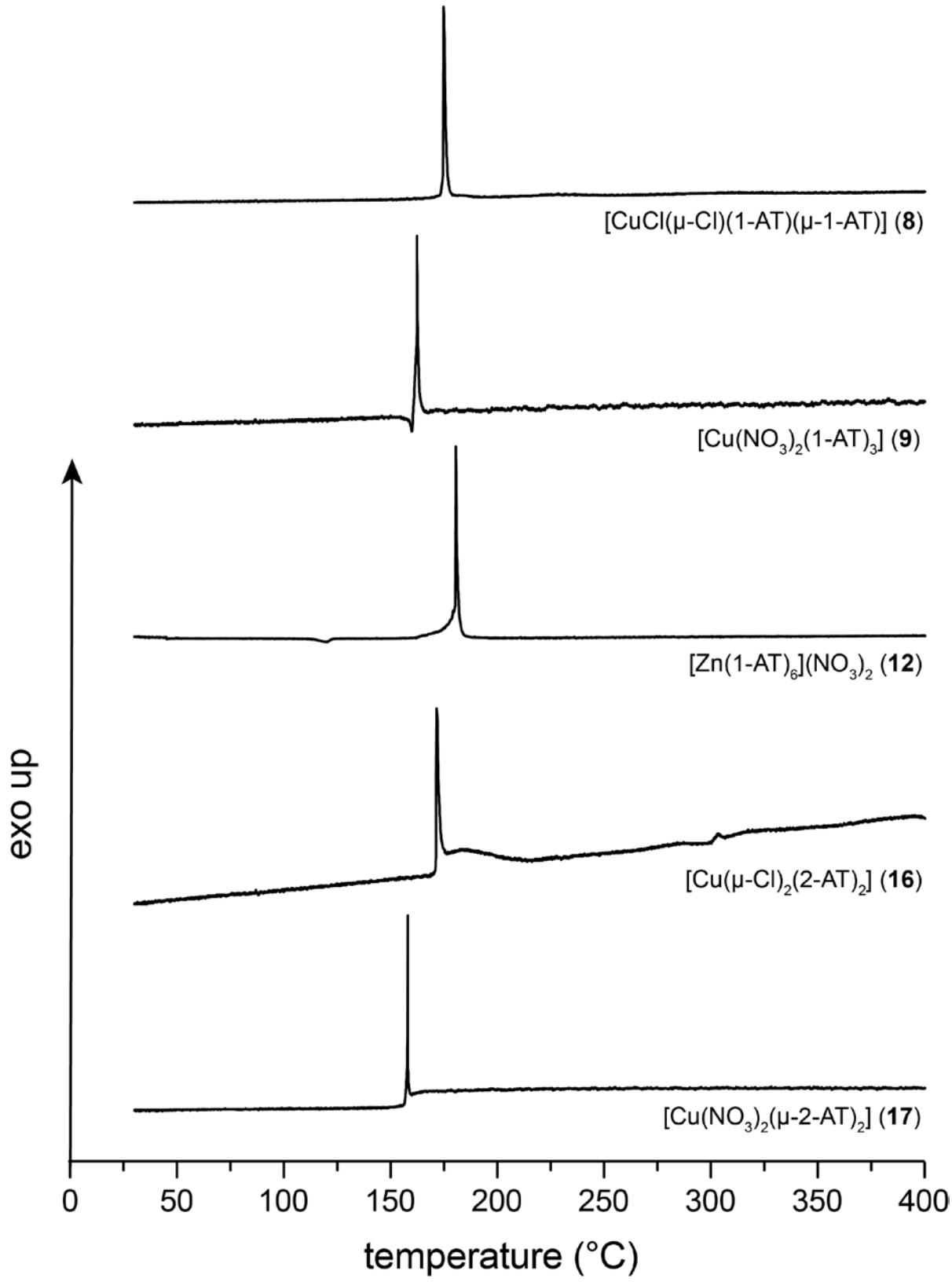

Figure S28 Different thermal analysis plots of **8**, **9**, **12**, **16**, and **17**.

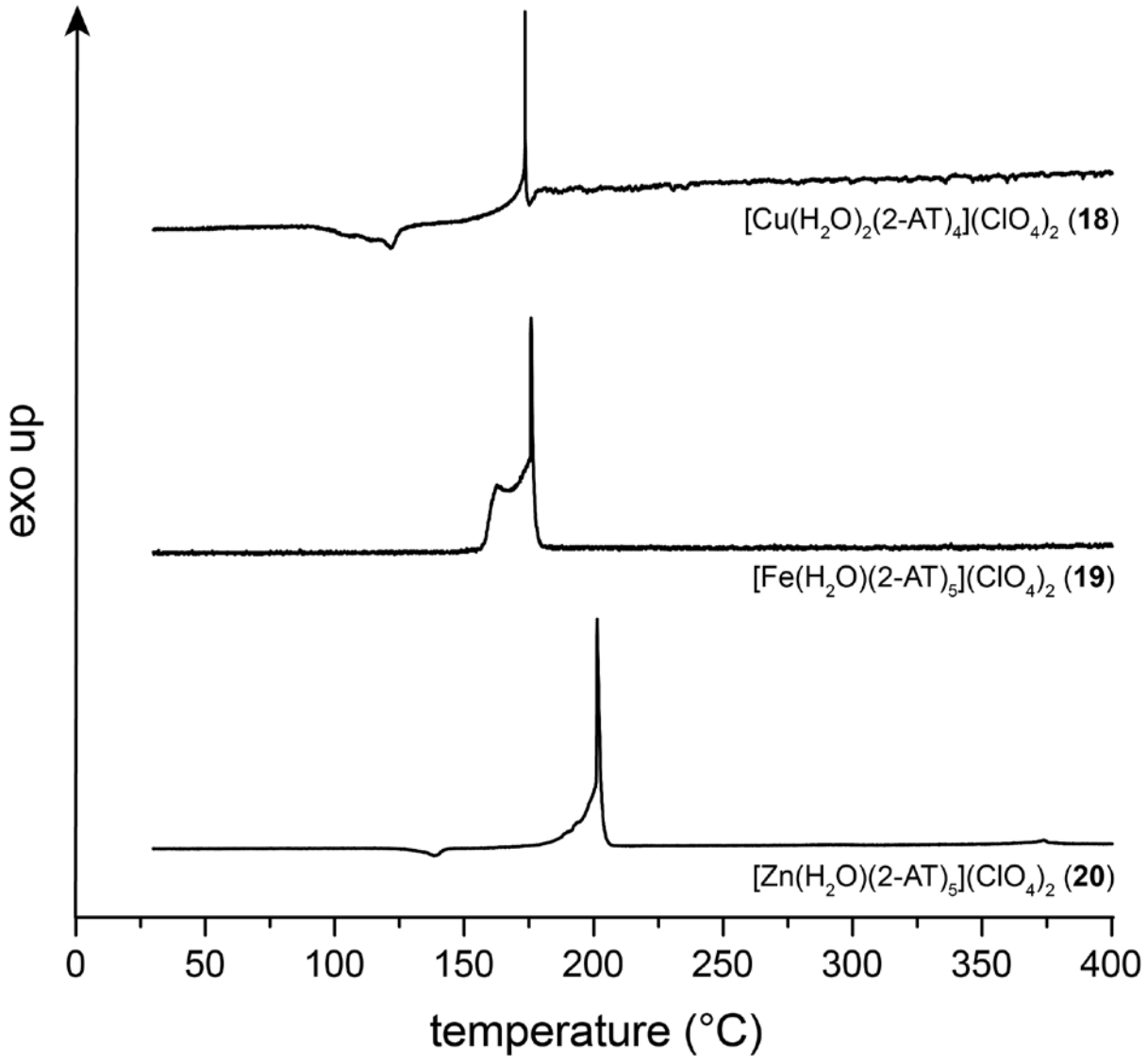

Figure S29 DTA plots of **18**–**20**.

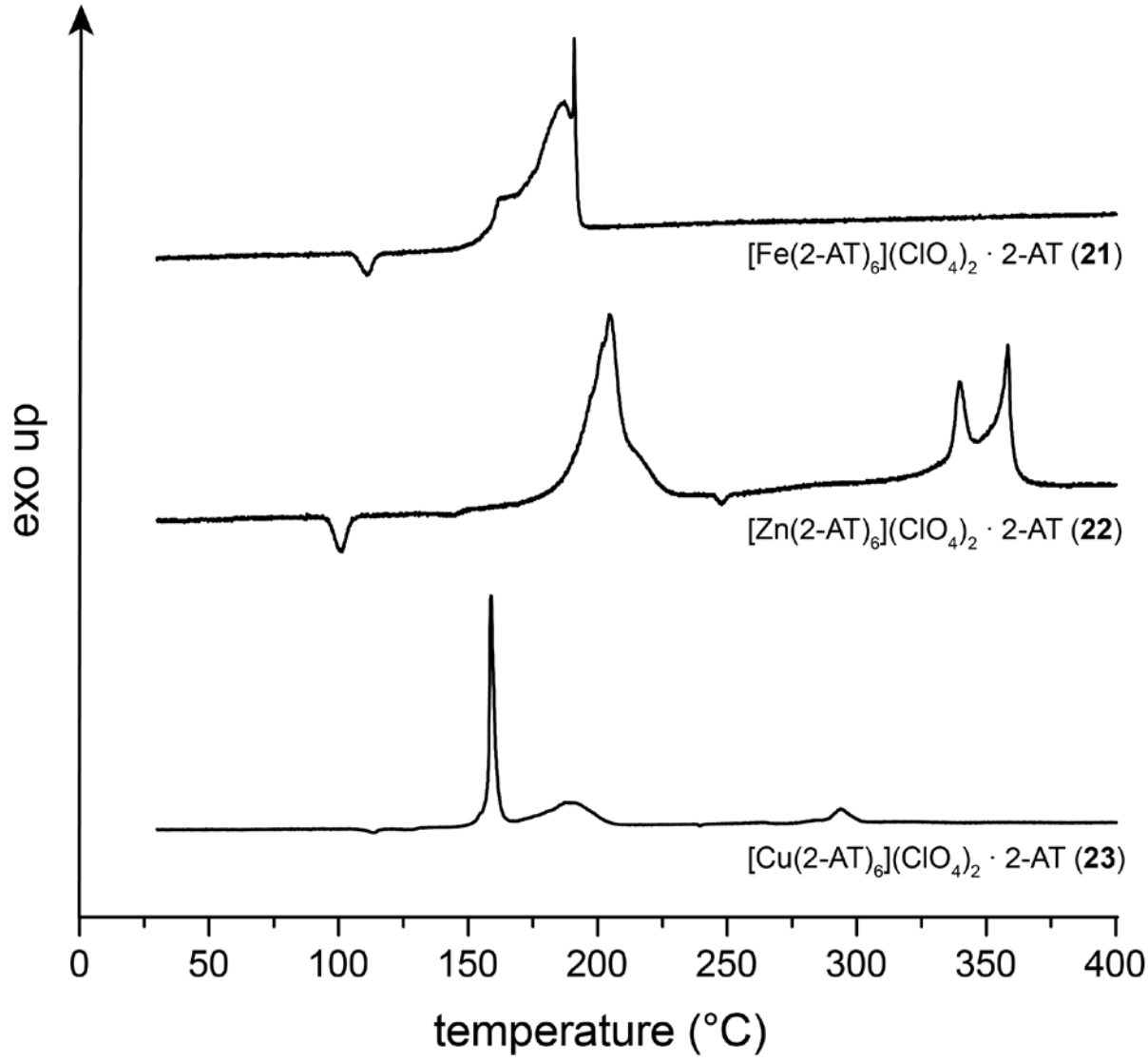

Figure S30 DTA plots of **21**–**23**.

6. Column diagrams of the complexes of 18–23

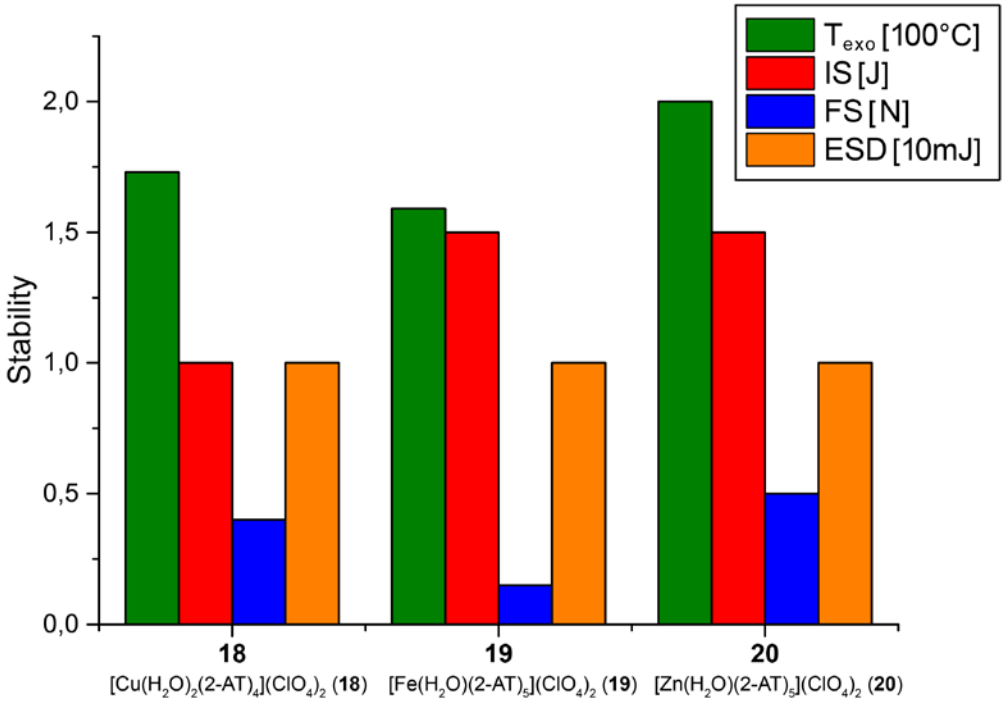

Figure S31 Stabilities of the aqua ligand containing metal(II) perchlorate complexes **18**–**20**.

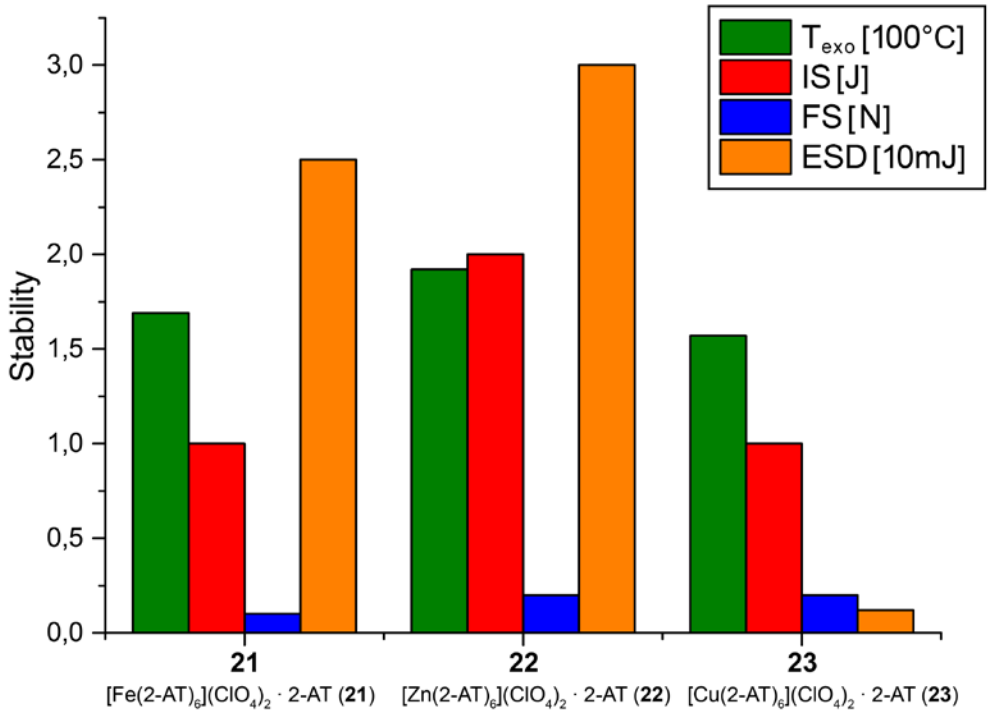

Figure S32 Stabilities of the 2-AT cocrystallized metal(II) perchlorate complexes **21**–**23**.

7. Hot plate and hot needle tests

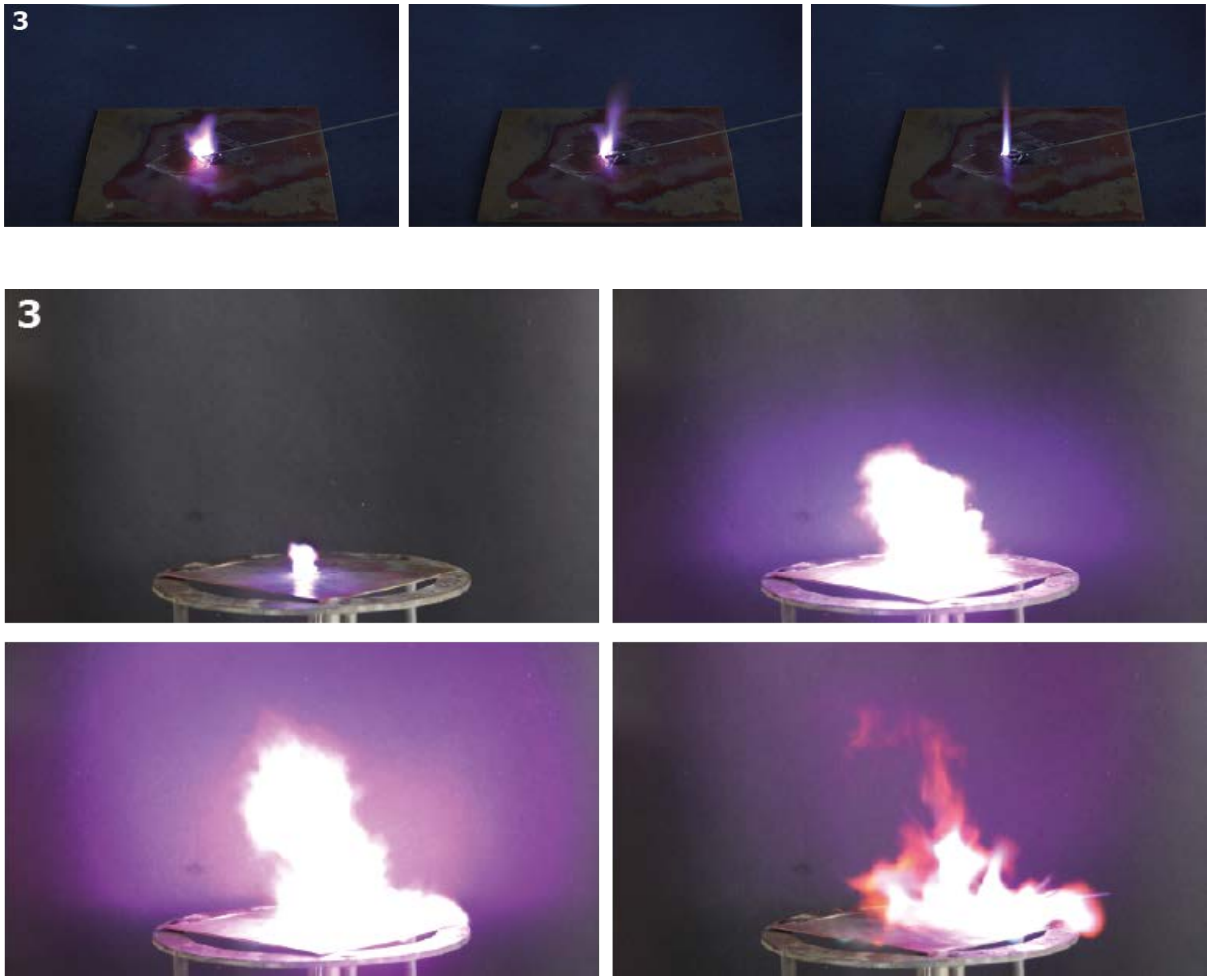

Figure S33 Hot needle and hot plate tests of complex **3** shown as a sequence.

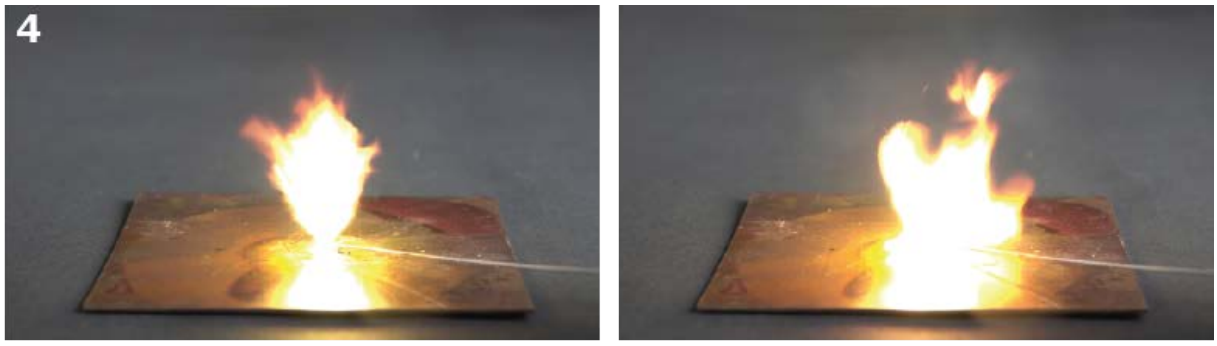

Figure S34 Hot needle test of coordination compound **4** shown as a sequence.

Figure S35 Hot plate test of coordination compound **4** shown as a sequence.

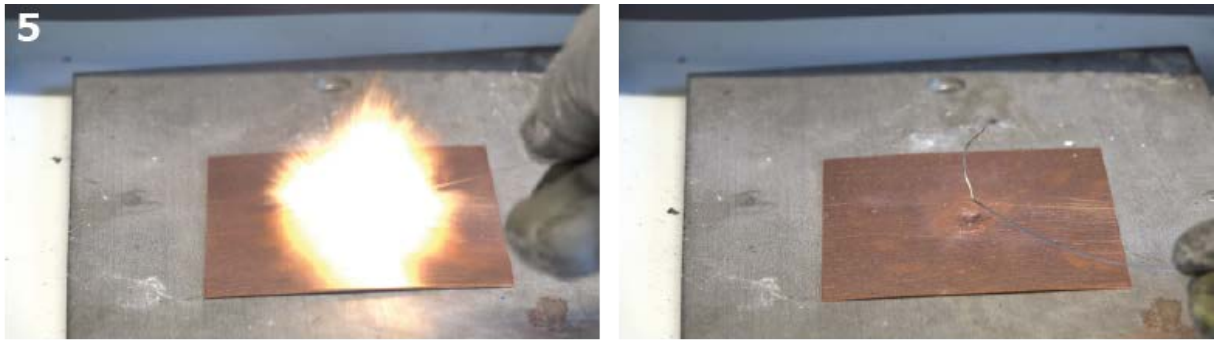

Figure S36 Detonation of coordination compound **5** during the hot needle and hot plate tests, partly shown as a sequence.

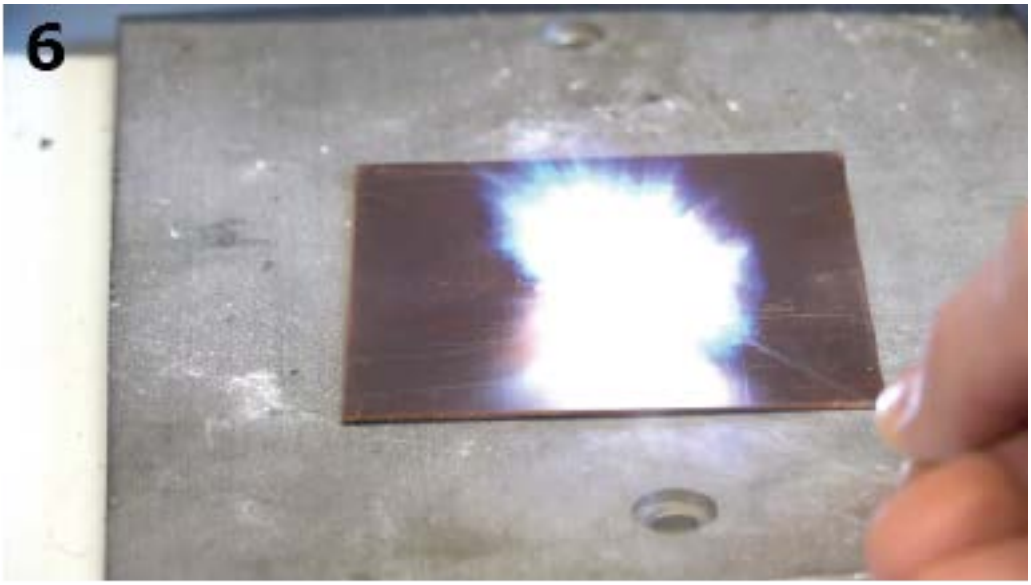

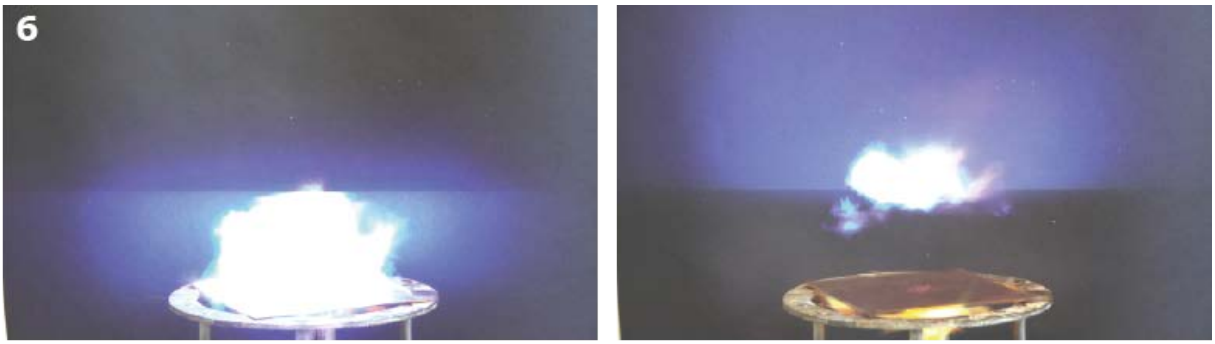

Figure S37 Detonation of coordination compound **6** during the hot needle and hot plate tests, partly shown as a sequence.

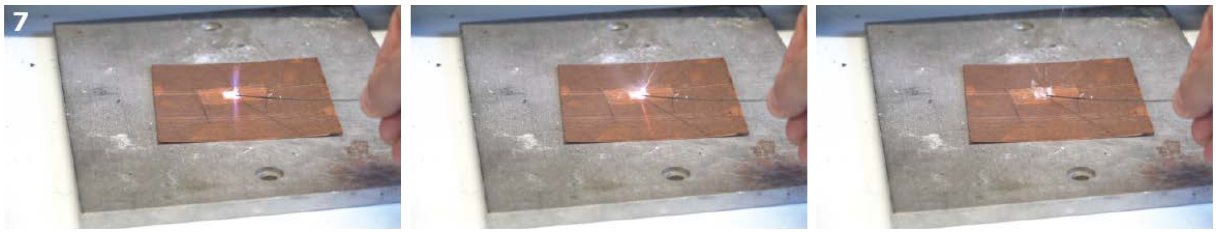

Figure S38 Initiation of complex **7** shown as a sequence during the hot needle test.

Figure S39 Hot plate test of complex **7** shown as a sequence.

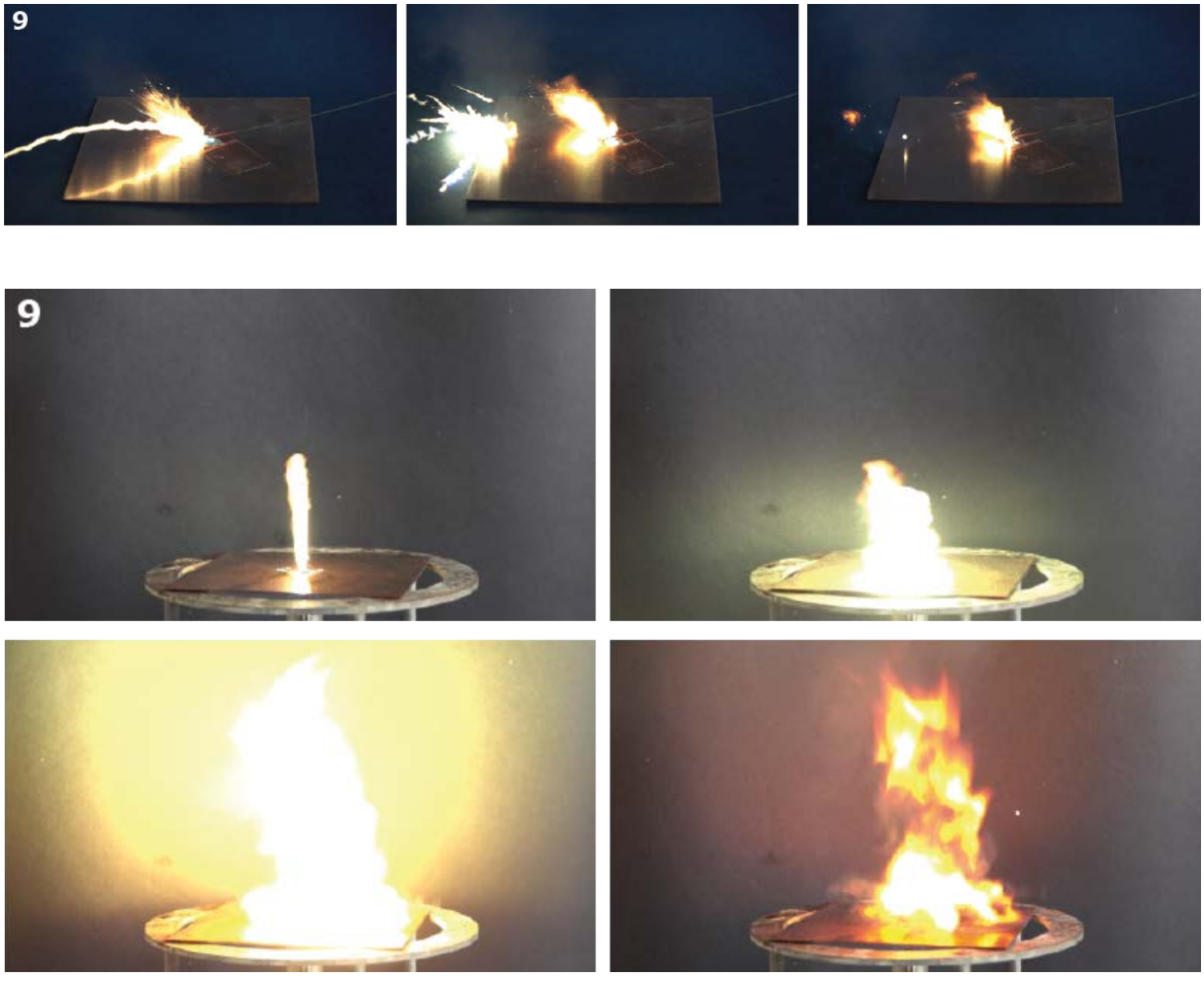

Figure S40 Hot needle and hot plate tests of the copper(II) nitrate complex **9** shown as sequences.

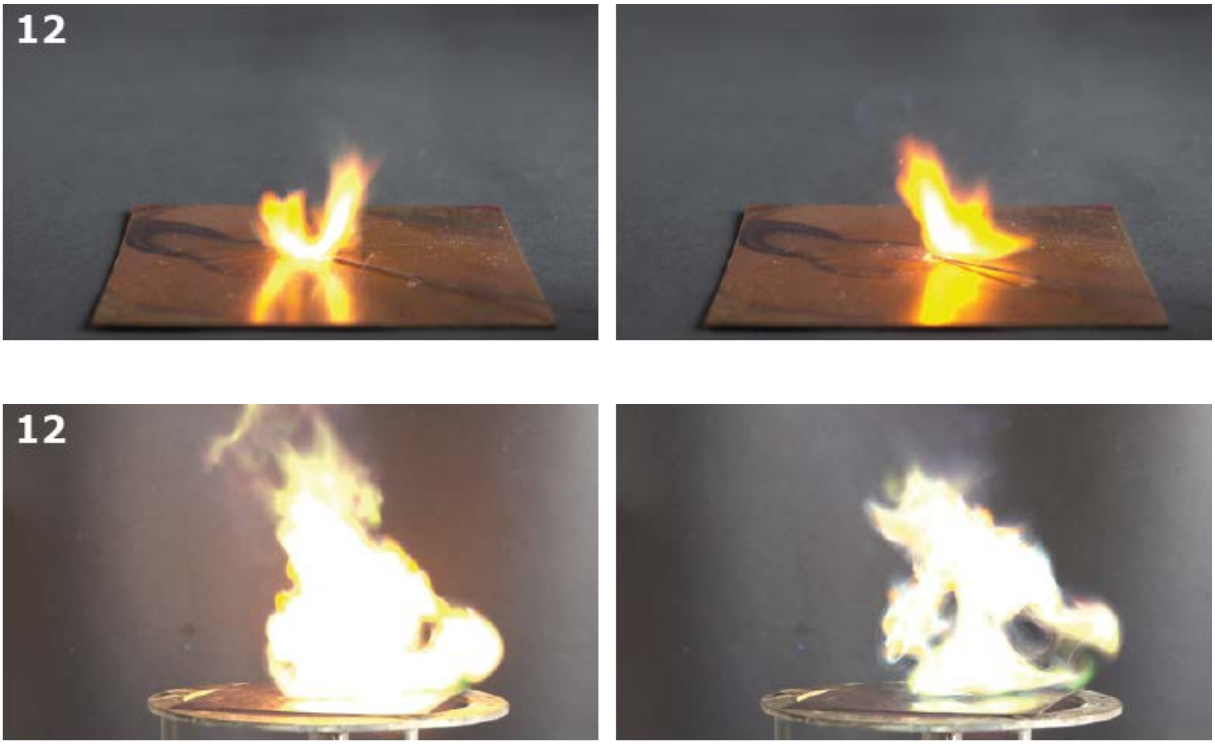

Figure S41 Initiation of the zinc(II) nitrate complex **12** shown as sequences during the hot needle and hot plate tests.

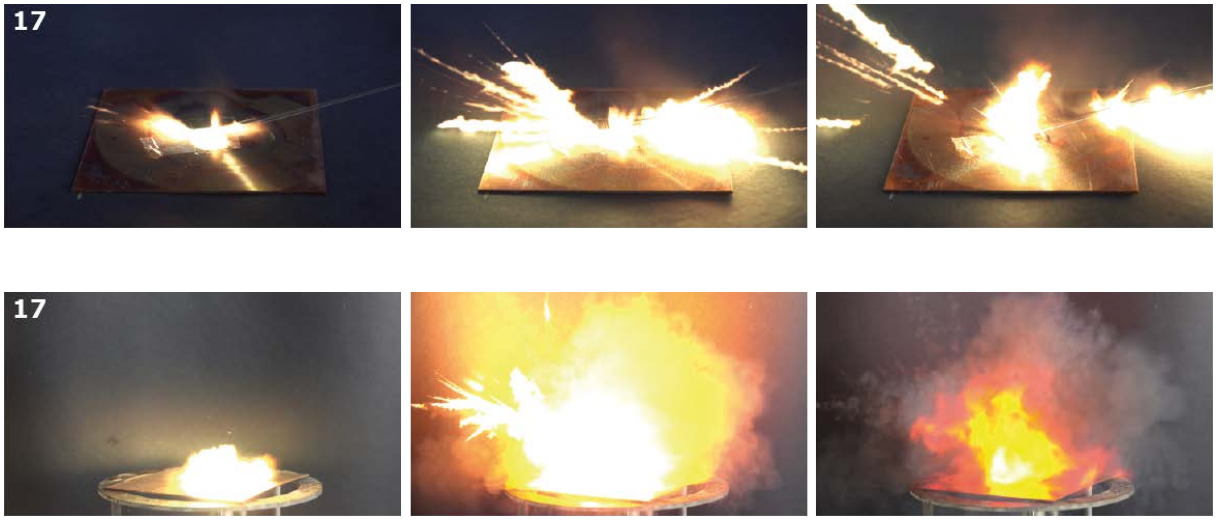

Figure S42 Imitations of the coordination compound **17** shown as sequences during the hot needle and hot plate tests.

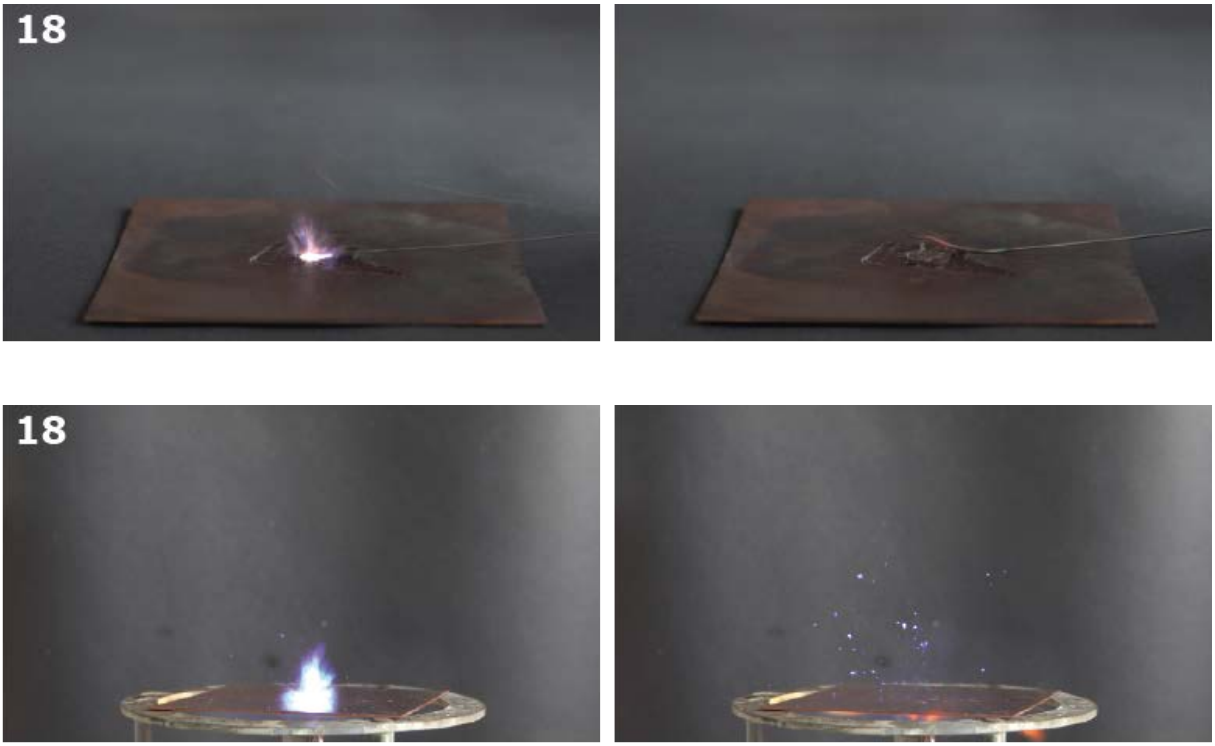

Figure S43 Detonations of the coordination compound **18** shown as sequences during the hot needle and hot plate tests.

Figure S44 Moment of detonation of complex **19** during the hot needle test.

Figure S45 Moment of detonation of complex **19** during the hot plate test.

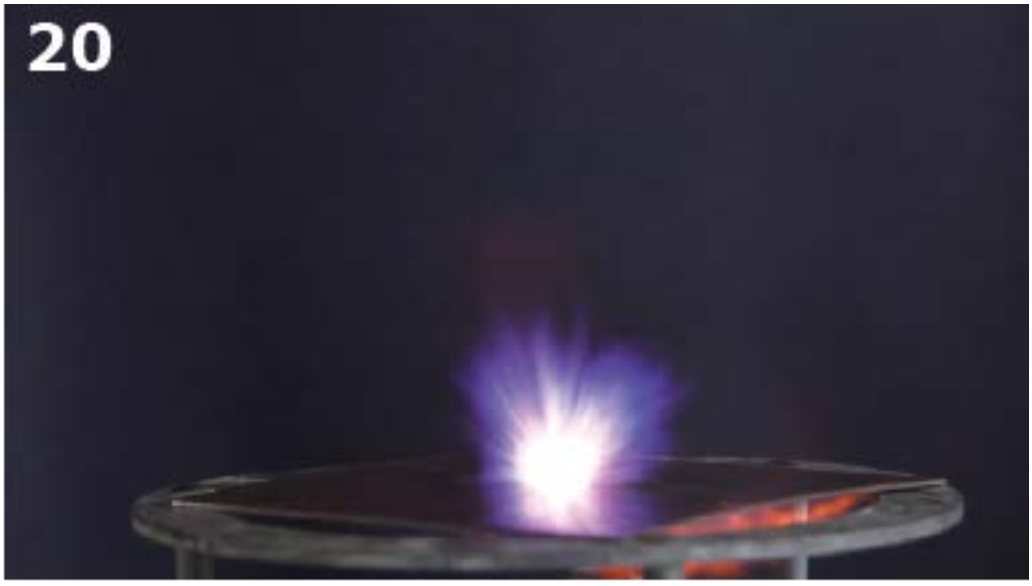

Figure S46 Detonation of complex **20** during the hot needle and hot plate tests, partly shown as a sequence.

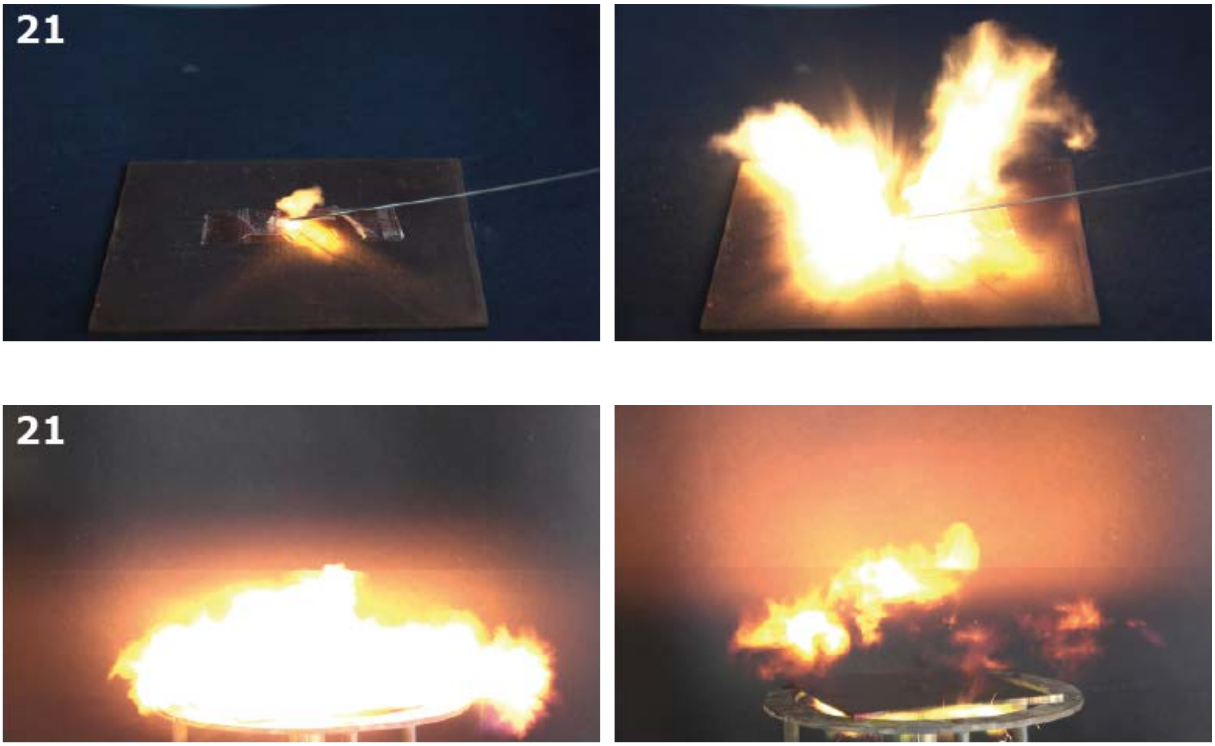

Figure S47 Detonations of coordination compound **21** during the hot needle and hot plate tests, partly shown as sequences.

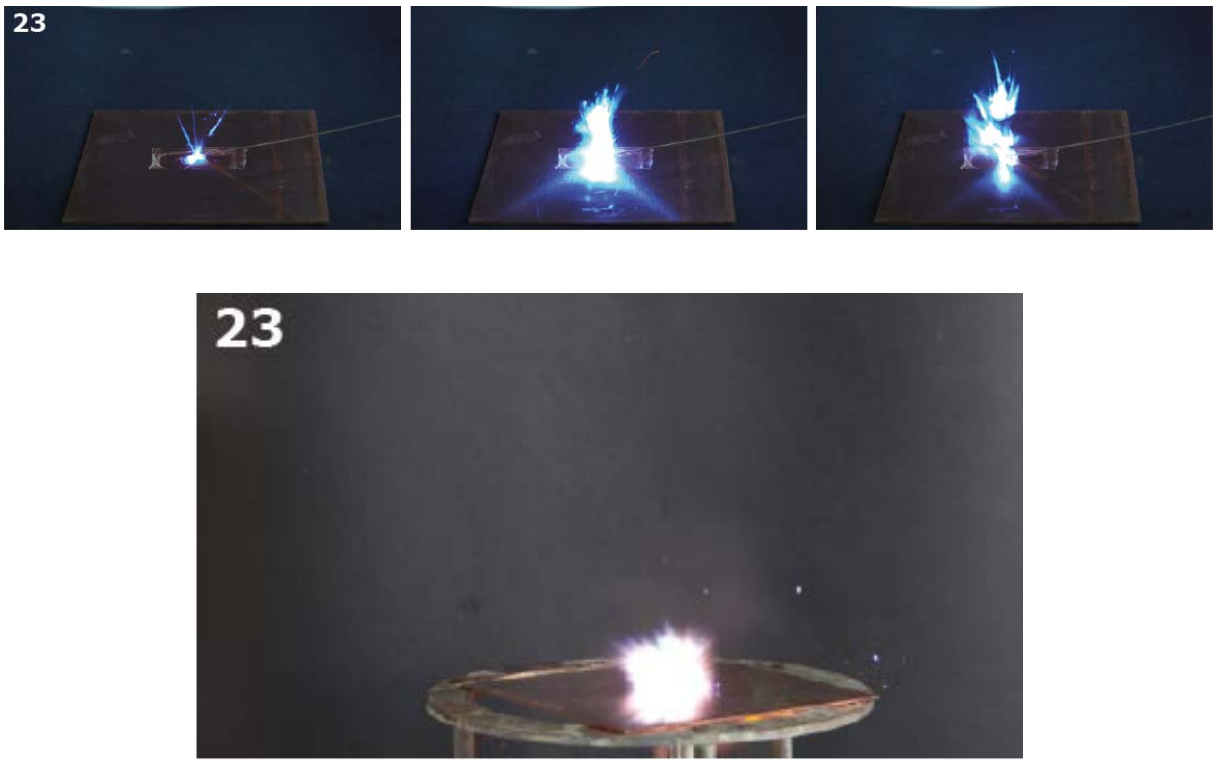

Figure S48 Behavior of complex **23** during the hot needle and hot plate tests, partly shown as a sequence.

8. Initiation capability tests

Figure S49 Positive PETN initiation test of 2-amino-5*H*-tetrazolium perchlorate salt **3**.

Figure S50 Positive PETN initiation tests of the copper(II) nitrate complexes **9** and **17**.

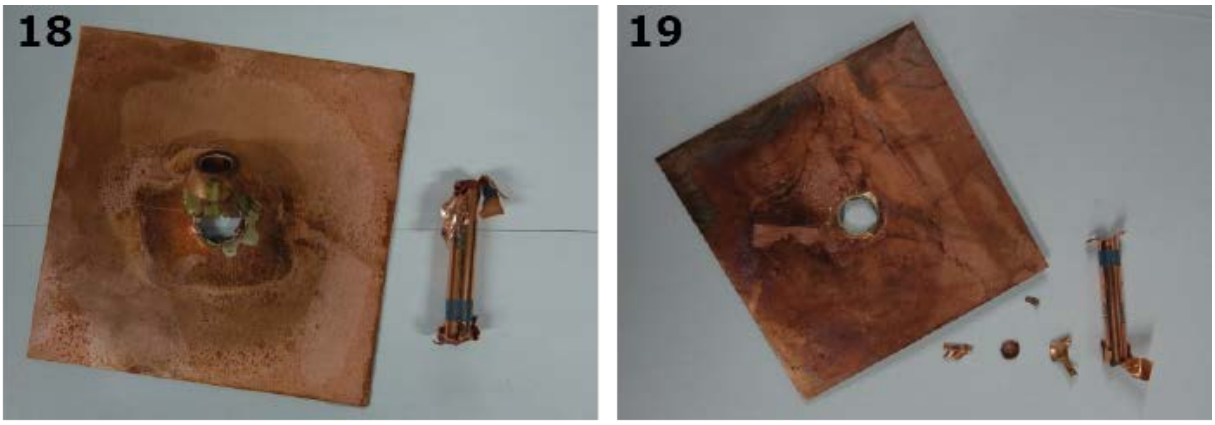

Figure S51 Positive PETN initiation tests of the metal(II) 2-AT perchlorate complexes **18** and **19**.

Figure S52 Positive PETN initiation tests of the 2-AT cocrystallized metal(II) perchlorate complexes **21**–**23**.

9. Laser ignition tests

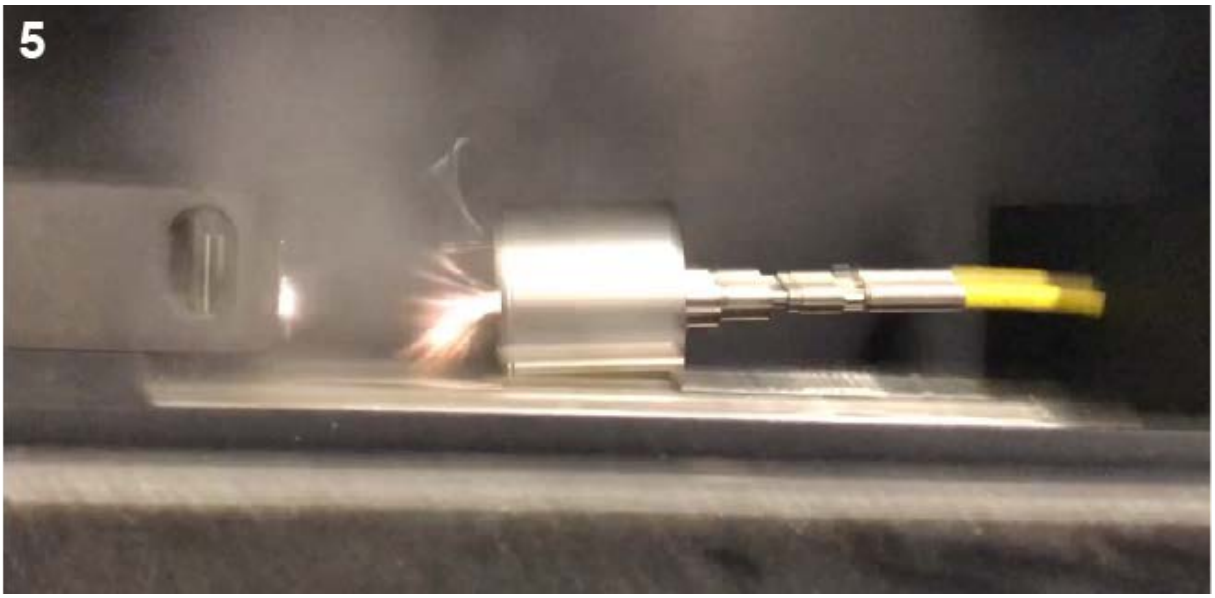

Figure S53 Detonation of **5** during the laser initiation test.

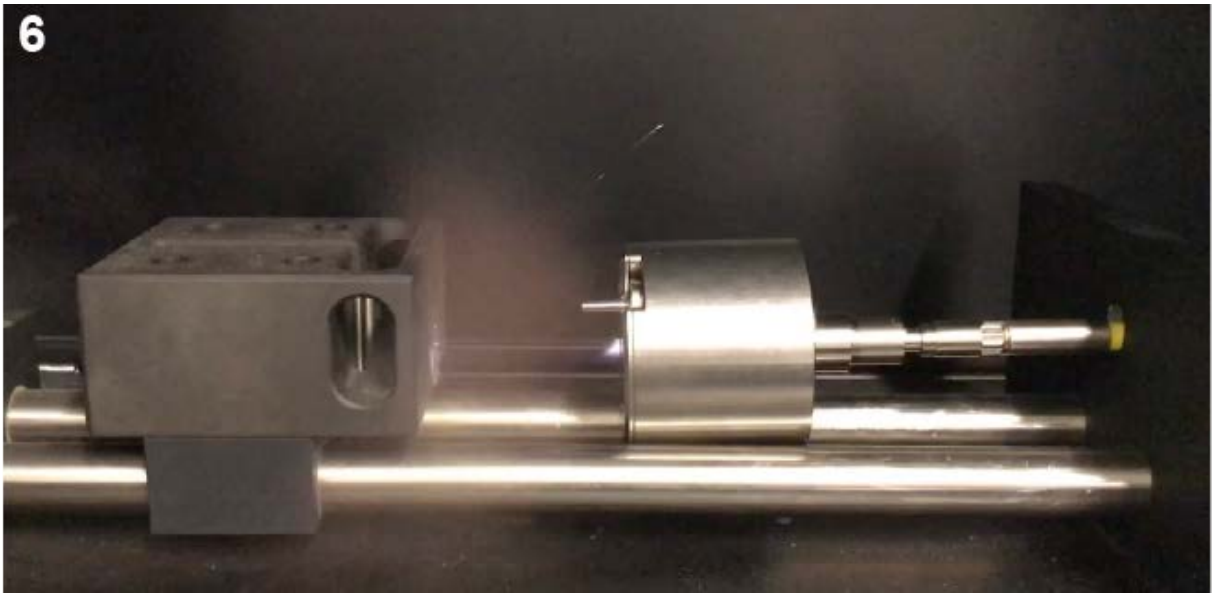

Figure S54 Detonation of **6** as reaction to laser irradiation.

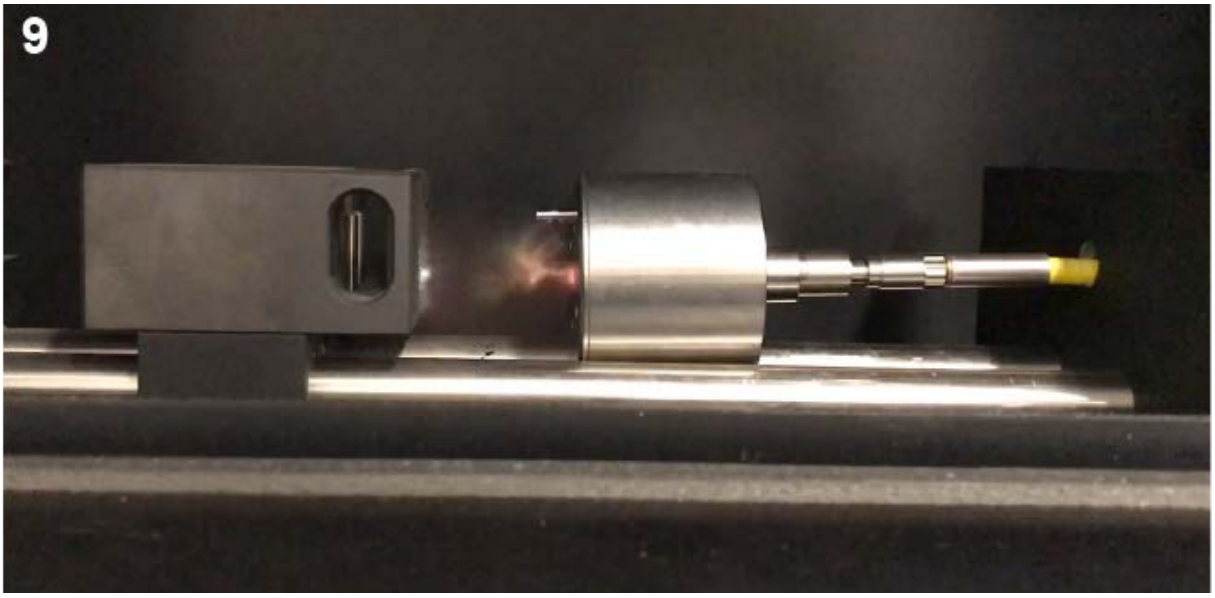

Figure S55 Moment of detonation of the copper(II) nitrate complex **9**.

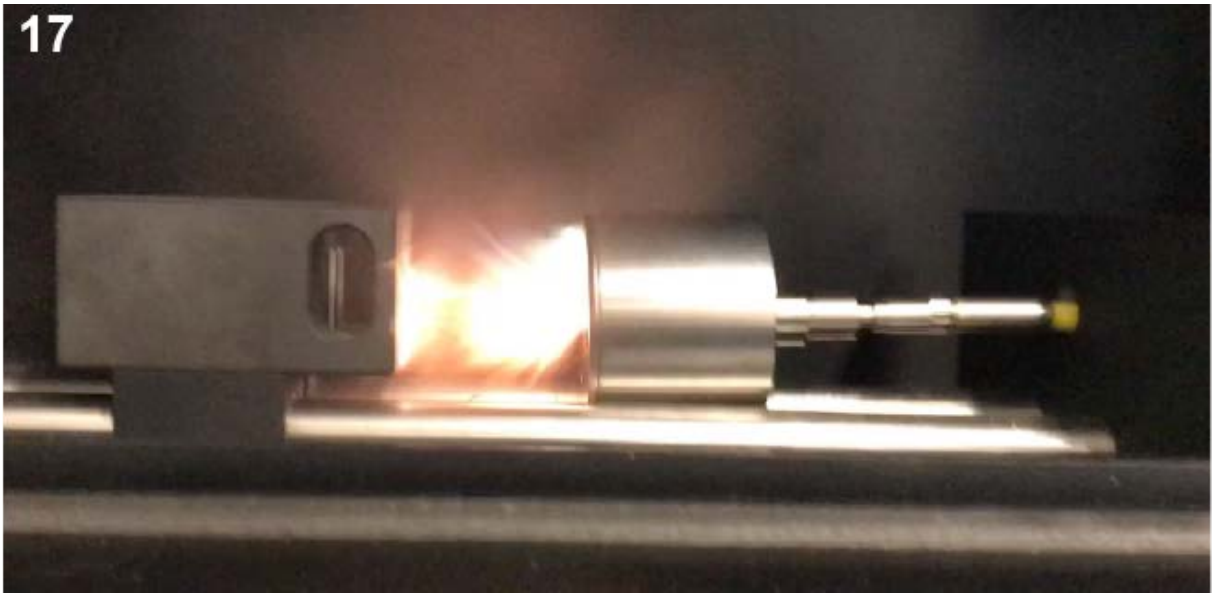

Figure S56 Detonation reaction of complex **17** during the laser initiation experiment.

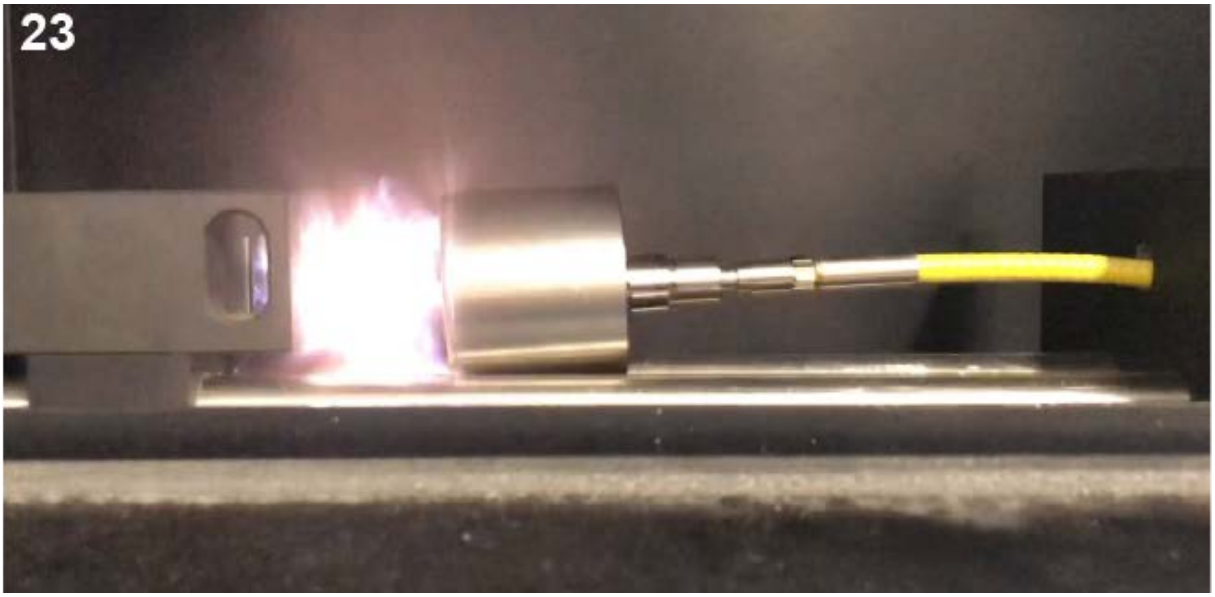

Figure S57 Moment of detonation of the copper(II) perchlorate complex **23**.

10. UV-Vis spectra of 18, 19, 21 and 23

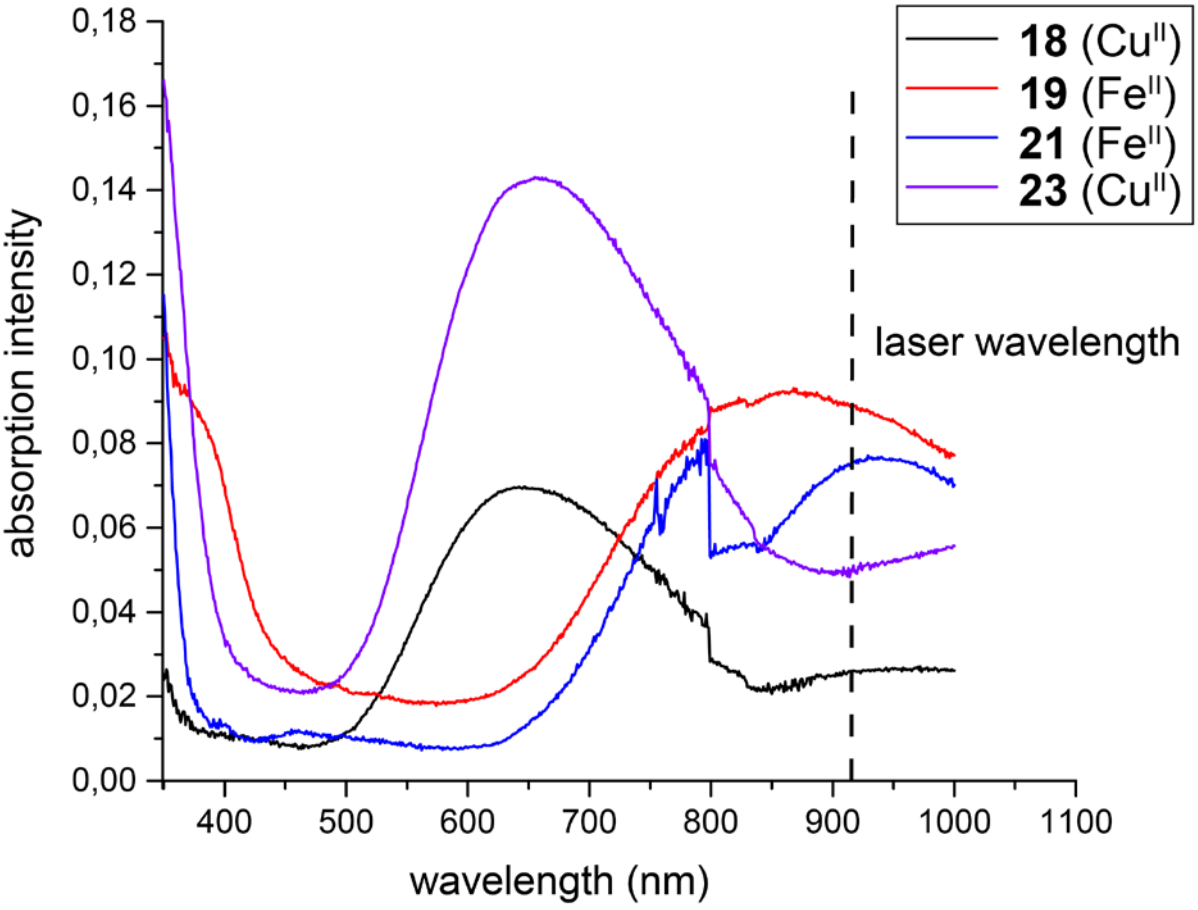

Figure S58 UV-Vis spectra in the solid state of coordination compounds **18**, **19**, **21**, and **23**.

11. Experimental part and general methods

All chemicals and solvents were employed as received (Sigma-Aldrich, Fluka, Acros, ABCR). The chemical composition and morphology of selected samples were investigated with a Scanning electron microscope (SEM) NanoLab G3 (Helios). The samples were carbon-coated (BAL-TEC MED 020, Bal Tec AG) to prevent electrostatic charging and to increase the conductivity. Energy dispersive X-ray spectroscopy (EDX) was carried out with an acceleration voltage of 20 kV using an X-Max 80 SDD detector (Oxford Instruments). ^{1}H, ^{13}C and ^{15}N spectra were recorded at ambient temperature using a JEOL Bruker 400, Eclipse 270, JEOL EX 400 or a JEOL Eclipse 400 instrument. The chemical shifts quoted in ppm in the text refer to

typical standards such as tetramethylsilane (^{1}H, ^{13}C) and nitromethane (^{15}N) in d_6-DMSO, *d*-$CHCl_3$ or d_3-MeCN as the solvents. The ^{1}H,^{15}N-HMBC NMR spectrum was measured with a data matrix of 1024 x 256, an applied zero filling of 2048 x 4096, 32 scans per round, a relaxation delay of 1 second, an acquisition time of 0.3 second at a concentration of 140 mg/mL and an overall measurement time of approx. 3 h. Endothermic and exothermic events of the described compounds, which indicate melting, evaporation or decomposition, are given as the extrapolated onset temperatures. The samples were measured in a range of 25–400 °C at a heating rate of 5 °C min^{-1} through differential thermal analysis (DTA) with an OZM Research DTA 552-Ex instrument and partly by thermal gravimetric analysis (TGA) with a PerkinElmer TGA4000. Infrared spectra were measured with pure samples on a Perkin-Elmer BXII FT-IR system with a Smith DuraSampler IR II diamond ATR. Determination of the carbon, hydrogen and nitrogen contents was carried out by combustion analysis using an Elementar Vario El (nitrogen values determined are often lower than those calculated due to their explosive behavior). UV-Vis spectra were recorded in the solid state using a Varian Cary 500 spectrometer in the wavelength range of 350–1000 nm. The step in the absorption intensity at 800 nm is caused by a detector change. Impact sensitivity tests were carried out according to STANAG 4489[S10] with a modified instruction[S11] using a BAM (Bundesanstalt für Materialforschung) drophammer.[S12,13] Ball drop impact sensitivities were determined for selected compounds on an OZM ball drop machine (BIT-132) following MIL-STD-1751A (method 1016) by dropping a free-falling steel ball onto the explosive compound.[S14] A sample of approximately 30 mg was placed on a steel block and spread into a 0.33 mm layer of substance. The steel ball guide was set to the desired height and the loaded impact block positioned underneath. By releasing the ball shield, a 0.500-inch steel ball, weighing 8.35 g, was allowed to fall onto the sample. Any visual observation of decomposition was regarded as a positive result. If no reaction occurred, the remaining substance was disposed, and the impact block loaded with a freshly prepared sample. The limiting impact energy was determined in

conformity with the recommended UN method for testing impact and friction sensitivities (1-in-6 approach), according to ST/SG/AC.10/11/Rev.6 (s. 13.4.2.3.3).[S15] The impact energy was calculated as the product of the weight of the steel ball and its fall height. An initial drop height was chosen, at which an explosion of the sample could be ensured. The impact energy level (ball guide height) was now stepwise decreased until no reaction was observed. At this point, testing was continued up to a total of six trials at that certain energy level. If an explosion occurred, the procedure was repeated by decreasing the drop height. As soon as six trials at a fixed energy level emerged as negative, the next higher energy level, where at least one out of at least six trials resulted in an explosion, is determined as the limiting impact energy. Friction sensitivity tests were carried out according to STANAG 4487[S16] with a modified instruction[S17] using the BAM friction tester. The classification of the tested compounds results from the "UN Recommendations on the Transport of Dangerous Goods".[S18] Additionally all compounds were tested to determine the sensitivity toward electrical discharge using the OZM Electric Spark Tester ESD 2010 EN or OZM Electric Spark XSpark10 device.[S11] Hot plate and hot needle tests were performed in order to classify the initiation capability of selected complexes. The samples were fixed on a copper plate underneath adhesive tape and initiated by a red hot needle. Strong deflagration or detonation of the compound usually indicates a valuable primary explosive. The safe and straightforward hot plate test only shows the behavior of the unconfined sample toward fast heating on a copper plate. It does not necessarily allow any conclusions on a compound´s capability as a suitable primary explosive. Initiation capability tests of the newly investigated complexes toward pentaerythritol tetranitrate (PETN) were carried out in a copper shell with a diameter of 7 mm and length of 88 mm filled with 200 mg of sieved secondary explosive (grain size < 100 µm). First, the secondary explosive was pressed with a weight of 8 kg, then the primary explosive to be investigated was subsequently filled on top of the main charge and pressed with the same pressure force. The shell was sealed by an insulator, placed in a retaining ring, which was soldered to a copper witness plate with a thickness of 1 mm and finally initiated

by a type A electric igniter. A positive test is indicated by a hole in the copper plate and fragmentation of the shell caused by a deflagration-to-detonation transition (DDT) of PETN. Liquid-dried luminescent bacteria of the strain *Vibrio fischeri* NRRL-B-11177 provided by the HACH LANGE GmbH were used for the luminescent bacteria inhibition test to determine their toxicity toward aquatic organisms according to a modified procedure.[S19] The laser initiation experiments were performed with a 45 W InGaAs laser diode operating in the single-pulsed mode. The diode is attached to an optical fiber with a core diameter of 400 μm and a cladding diameter of 480 μm. The optical fiber is connected via a SMA type connecter directly to the laser and to a collimator. This collimator is coupled to an optical lens, which was positioned in its focal distance (f = 29.9 mm) to the sample. The lens is shielded from the explosive by a sapphire glass. Approximately 15 mg of the carefully pestled complex to be investigated was filled into a transparent plastic cap (PC), pressed with a pressure force of 1 kN and sealed by a UV-curing adhesive. The confined samples were irradiated at a wavelength of 915 nm, a voltage of 4 V, currents of 6–8 A and varying pulse lengths (0.1 ms or 15 ms). The combined currents and pulse lengths result in an energy output of about 0.15 mJ up to 27 mJ.

The obtained coordination compounds were washed with cold ethanol when stated, dried overnight in air and used for analytics without further purification.

CAUTION! *All investigated compounds are potentially explosive energetic materials (the majority of the compounds lie in the range of primary explosives), which show partly increased sensitivities toward various stimuli (e.g. elevated temperatures, impact, friction or electrostatic discharge). Therefore, proper security precautions (safety glasses, face shield, earthed equipment and shoes, leather jacket, Kevlar gloves, Kevlar sleeves and ear plugs) have to be worn while synthesizing and handling the described compounds. Especially the very sensitive compounds* ***4–7*** *and* ***18–23*** *must be handled with great care! An excess of ligand* ***2*** *has to be applied during the synthesis of complex* ***18*** *in order to prevent the formation of unisolable side*

species (most likely a diperchlorato or hexacoordinated tetrazole complex), which tends to spontaneous violent decomposition during crystallization.

Procedure for the preparation of 1-amino-5*H*-tetrazole (1) and 2-amino-5*H*-tetrazole (2):

Selective 1-amino-5*H*-tetrazole (1) synthesis:

Hydrazine monohydrate (46.2 mL, 940 mmol) was dissolved in 200 ml ethanol and the mixture cooled to 0 °C with an ice bath. Under vigorous stirring benzaldehyde (24 mL, 236 mmol) was added dropwise over a time period of 5 minutes. After complete addition, the resulting mixture was further stirred for 1 min at this temperature before quenching with water (300 mL). The milky white aqueous phase was extracted with dichloromethane (3 x 300 mL) and the combined organic phases dried over $MgSO_4$. The solvent was removed under reduced pressure yielding benzhydrazone in form of a yellow, odorous oil (20.8 g, 193 mmol, 82 %). ^{1}H NMR ($CHCl_3$-*d*, 25 °C, ppm) δ: 7.71 (s, 1H, NC-*H*), 7.54–7.49 (m, 2H, C_{aromat}-*H*), 7.36–7.23 (m, 3H, C_{aromat}-*H*), 5.48 (s, 2H, -N*H*$_2$). Benzhydrazone (20.8 g, 193 mmol) was dissolved in triethyl orthoformate (60 mL, 364 mmol) and subsequently further reacted with sodium azide (16.0 g, 246 mmol). While stirring, glacial acetic acid (100 mL) was added dropwise and the resulting reaction mixture heated to 80 °C for 2.5 h. During the reaction, a color change from yellow to orange and finally red could be observed. After complete reaction, the warm mixture was poured into water (200 mL) and stirred overnight. The yellow precipitate formed was filtrated, washed with a small amount of water and dried overnight in air yielding 1-benzylideneaminotetrazole (13.2 g, 76.2 mmol, 40 %). ^{1}H NMR ($CHCl_3$-*d*, 25 °C, ppm) δ: 9.37 (s, 1H, N_4C-*H*), 8.87 (s, 1H, NC-*H*), 7.96–7.84 (m, 2H, C_{aromat}-*H*), 7.67–7.47 (m, 3H, C_{aromat}-*H*). Under vigorous stirring, concentrated hydrochloric acid (150 mL) was added to 1-benzylideneaminotetrazole (13.2 g, 76.2 mmol) and water (200 mL). The suspension obtained was refluxed for 30 min resulting in a clear yellow solution. The cleaved benzaldehyde was

removed together with the solvent in vacuo at 80 °C and the residues checked by TLC upon reaction completion. The received yellow-white residue was neutralized with a saturated solution of $NaHCO_3$ and extracted with EtOAc (3 x 400 mL). The combined organic phases were dried over $MgSO_4$ and the solvent removed under reduced pressure, yielding 1-amino-5*H*-tetrazole (**1**, 6.40 g, 75.2 mmol, 99 %) in form of a yellow liquid.

Amination of 1,5*H*-tetrazole:

The performed synthesis of the two isomers was carried out analogous to a modified literature procedure.[S20] 1,5-*H*-Tetrazole (14.0 g, 200 mmol) was dissolved in water (150 mL) and treated with Na_2CO_3 (23.2 g, 219 mmol). The resulting solution was heated to 75 °C, followed by the dropwise addition of hydroxylamine-*O*-sulfonic acid (27.2 g, 240 mmol) in water (120 mL). In the meantime, the pH value of the solution was maintained between 7 and 8 by periodic addition of a saturated solution of $NaHCO_3$. The reaction mixture was refluxed for 30 minutes followed by the evaporation of approximately half of the solvent under reduced pressure. After continuously extracting the remaining solution with ethyl acetate for two days, the evaporation of the extract gave a viscous oil containing both isomers **1** and **2**. The isomers were separated by column chromatography (SiO_2, ethyl acetate/ dichloromethane 5:1, R_f = 0.71, 0.47) yielding highly pure 2-amino-5*H*-tetrazole (**2**, 3.17 g, 37.2 mmol, 19 %) and 1-amino-5*H*-tetrazole (**1**, 4.54 g, 53.4 mmol, 27 %) as colorless liquids.

1-Amino-5*H*-tetrazole (1)

DTA (5 °C min^{-1}): 182 °C (exothermic); IR (ATR, cm^{-1}): $\tilde{\nu}$ = 3326 (m), 3197 (m), 3144 (m), 1626 (m), 1491 (w), 1430 (w), 1342 (w), 1273 (w), 1185 (s), 1098 (vs), 962 (s), 871 (s), 723 (m), 695 (m), 643 (vs); ^{1}H NMR (DMSO-d_6, 25 °C, ppm) δ: 9.24 (s, 1H, C-*H*), 7.10 (s, 2H, -N*H*$_2$); ^{13}C NMR (DMSO-d_6, 25 °C, ppm) δ: 143.4 (-*C*N$_4$); ^{15}N NMR (MeCN-d_3, 25 °C, ppm)

δ: 6.8 (N3), −10.0 (N2), −53.8 (N4, d, $^{2}J_{N\text{-}H}$ = 11.2 Hz), −138.0 (N1, d, $^{2}J_{N\text{-}H}$ = 8.4 Hz), −308.4 (N5, t, $J_{N\text{-}H}$ = 73.1 Hz); EA: (CH_3N_5, 85.07) calcd: C 14.12, H 3.55, N 82.33 %; found: C 14.60, H 3.63, N 82.16 %.

2-Amino-5*H*-tetrazole (2)

DTA (5 °C min^{-1}): 197 °C (exothermic); IR (ATR, cm^{-1}): $\tilde{\nu}$ = 3314 (m), 3144 (m), 3128 (m), 3083 (w), 3012 (w), 2978 (w), 1685 (w), 1613 (m), 1488 (m),1451 (m), 1434 (m), 1388 (w), 1374 (w), 1361 (w), 1285 (s), 1259 (w), 1218 (m), 1174 (s), 1141 (s), 1111 (s), 1103 (s), 1064 (m), 1024 (s), 992 (s), 975 (s), 928 (s), 876 (s), 803 (w), 797 (w), 745 (m), 722 (m), 704 (s), 680 (m), 666 (vs), 644 (m); ^{1}H NMR (DMSO-d_6, 25 °C, ppm) δ: 8.72 (s, 1H, C-*H*), 8.03 (s, 2H, -NH_2); ^{13}C NMR (DMSO-d_6, 25 °C, ppm) δ: 151.8 (-CN$_4$); ^{15}N NMR (MeCN-d_3, 25 °C, ppm) δ: −11.2 (N3), −53.9 (N4, d, $^{2}J_{N\text{-}H}$ = 12.2 Hz), −78.9 (N1, d, $^{2}J_{N\text{-}H}$ = 14.5 Hz), −92.6 (N2, d, $^{2}J_{N\text{-}H}$ = 7.9 Hz), −289.6 (N5, t, $J_{N\text{-}H}$ = 72.5 Hz); EA: (CH_3N_5, 85.07) calcd: C 14.12, H 3.55, N 82.33 %; found: C 14.45, H 3.58, N 82.26 %.

2-Amino-5*H*-tetrazolium perchlorate (3)

2-Aminotetrazole (**2,** 255 mg, 3.00 mmol) was added to perchloric acid (1 M, 3 mL, 3.00 mmol) and mechanically stirred for 30 minutes. The obtained solution was left for crystallization at room temperature. After five days, the received colorless crystals were filtered and washed with diethyl ether to stoichiometrically yield 2-amino-5*H*-tetrazolium perchlorate (**3**).

DTA (5 °C min^{-1}): 122 °C (endothermic, followed by exothermic); IR (ATR, cm^{-1}): $\tilde{\nu}$ = 3332 (m), 3253 (m), 3147 (m), 3009 (w), 2967 (w), 2924 (w), 2883 (w), 2792 (w), 2755 (w), 1600

(w), 1530 (m), 1493 (w), 1451 (m), 1401 (w), 1269 (w), 1136 (m), 1107 (s), 1040 (s), 1004 (s), 984 (s), 904 (s), 775 (s), 713 (s), 698 (s), 649 (s), 635 (s), 617 (vs); EA: ($CH_4ClN_5O_4$, 185.52): calcd: C 6.47, H 2.17, N 37.45 %; found: C 6.47, H 2.37, N 37.45 %; BAM drophammer: < 1 J; friction tester: 0.2 N; ESD: 10 mJ (at grain size < 100 μm).

General procedure for the preparation of metal(II) (Mn^{II}, Fe^{II}, Cu^{II}, Zn^{II}) 1-AT perchlorate complexes (4–7):

1-Amino-5*H*-tetrazole (**1**, 128 mg, 1.50 mmol) was dissolved in water (2 mL) and added dropwise to an aqueous solution (1 mL) of the corresponding metal(II) perchlorate (**4**: $Mn(ClO_4)_2 \cdot 6\ H_2O$ (91.0 mg, 0.25 mmol), **5**: $Fe(ClO_4)_2 \cdot 6\ H_2O$ (63.7 mg, 0.25 mmol) **6**: $Cu(ClO_4)_2 \cdot 6\ H_2O$ (92.6 mg, 0.25 mmol), **7**: $Zn(ClO_4)_2 \cdot 6\ H_2O$ (93.1 mg, 0.25 mmol). The colored reaction mixtures were mechanically stirred for one minute at ambient temperature and left for crystallization. After crystallization, the products were filtered off, washed (except complex **4**, due to its good solubility in ethanol) and dried in air.

$[Mn(1\text{-}AT)_6](ClO_4)_2$ (4)

The manganese(II) complex **4** crystallized within 4 days in the form of colorless rods suitable for X-ray determination. Yield: 142 mg (0.18 mmol, 72 %).

DTA (5 °C min^{-1}): 195 °C (exothermic); IR (ATR, cm^{-1}): $\tilde{\nu}$ = 3617 (vw), 3345 (m), 3293 (w), 3231 (w), 3142 (m), 1626 (m), 1506 (vw), 1439 (w), 1302 (w), 1194 (m), 1177 (w), 1092(vs), 1071 (vs), 984 (s), 934 (m), 869 (m), 721 (w), 700 (m), 644 (s), 622 (s); EA: ($C_6H_6Cl_2MnN_{30}O_8$, 764.25): calcd: C 9.43, H 2.37, N 54.98 %; found: C 9.85, H 2.35, N 54.39 %; ball drop impact tester: 14 mJ; BAM drophammer: < 1 J; friction tester: 0.5 N; ESD: 11 mJ (at grain size 100–500 μm).

$[Fe(1\text{-}AT)_6](ClO_4)_2$ (5)

Coordination compound **5** was obtained within three days in the form of colorless blocks suitable for X-ray diffraction. Yield: 117 mg (0.15 mmol, 60 %).

DTA (5 °C min^{-1}): 187 °C (exothermic); IR (ATR, cm^{-1}): $\tilde{\nu}$ = 3347 (w), 3295 (w), 3232 (w), 3145 (w), 1626 (m), 1508 (vw), 1440 (w), 1303 (w), 1195 (m), 1178 (w), 1092 (vs), 1074 (vs), 987 (s), 935 (m), 868 (m), 721 (w), 700 (m), 645 (m), 622 (s); UV-Vis spectrum: λ_{max} = 871 nm; EA: ($C_6H_{18}Cl_2FeN_{30}O_8$, 765.16): calcd: C 9.42, H 2.37, N 54.92 %; found: C 9.99, H 2.42, N 54.27 %; ball drop impact tester: 25 mJ; BAM drophammer: < 1 J; friction tester: < 0.1 N; ESD: 12 mJ (at grain size 100–500 μm).

$[Cu(1\text{-}AT)_6](ClO_4)_2$ (6)

Within a few hours, the very promising copper(II) complex **6** could be isolated in the form of blue blocks suitable for X-ray determination. Yield: 66.1 mg (0.09 mmol, 36 %).

DTA (5 °C min^{-1}): 174 °C (exothermic); IR (ATR, cm^{-1}): $\tilde{\nu}$ = 3346 (w), 3293 (w), 3229 (w), 3146 (w), 3010 (vw), 1626 (w), 1506 (vw), 1441 (w), 1340 (vw), 1308 (vw), 1194 (w), 1179 (w), 1090 (vs), 1074 (vs), 999 (m), 978 (m), 934 (m), 868 (m), 720 (w), 699 (m), 645 (s), 622 (s); UV-Vis spectrum: λ_{max} = 677 nm; EA: ($C_6H_{18}Cl_2CuN_{30}O_8$, 772.86): calcd: C 9.32, H 2.35, N 54.37 %; found: C 9.95, H 2.40, N 53.38 %; ball drop impact tester: < 4 mJ; BAM drophammer: < 1 J; friction tester: < 0.1 N; ESD: 5 mJ (at grain size < 100 μm).

$[Zn(1\text{-}AT)_6](ClO_4)_2$ (7)

After three days, the zinc perchlorate complex **7** was isolated in the form of colorless blocks suitable for X-ray diffraction. Yield: 64.2 mg (0.08 mmol, 32 %).

DTA (5 °C min^{-1}): 189 °C (exothermic); IR (ATR, cm^{-1}): $\tilde{\nu}$ = 3378 (w), 3347 (w), 3296 (w), 3231 (w), 3145 (w), 1625 (w), 1507 (vw), 1441 (w), 1340 (vw), 1302 (w), 1195 (m), 1178 (w), 1093 (vs), 1075 (vs), 989 (s), 935 (m), 868 (m), 758 (vw), 721 (w), 700 (m), 663 (vw), 645 (m), 623 (s); EA: ($C_6H_{18}Cl_2ZnN_{30}O_8$, 774.69): calcd: C 9.30, H 2.34, N 54.24 %; found: C 10.07, H 2.37, N 53.49 %; ball drop impact tester: 16 mJ; BAM drophammer: < 1 J; friction tester: 0.5 N; ESD: 12 mJ (at grain size 100–500 μm).

[CuCl(μ-Cl)(1-AT)(μ-1-AT)] (8)

1-Amino-5*H*-tetrazole (**1**, 42.5 mg, 0.50 mmol) was dissolved in ethanol (2 mL) and slowly added to an ethanolic solution (1 mL) of $CuCl_2 \cdot 2\ H_2O$ (42.6 mg, 0.25 mmol) while stirring mechanically. The obtained reaction mixture began to cloud leading to a green precipitate. The addition of 2 M HCl (1 mL) caused the precipitate to dissolve while stirring for 10 minutes. After only one day, [CuCl(μ-Cl)(1-AT)(μ-1-AT)] (**8**) was received in the form of green single crystals suitable for X-ray diffraction. Yield: 55.1 mg (0.18 mmol, 72 %).

DTA (5 °C min^{-1}) onset: 175 °C (exothermic); IR (ATR, cm^{-1}): $\tilde{\nu}$ = 3316 (w), 3263 (m), 3183 (m), 3155 (m), 3125 (m), 2956 (w), 1630 (w), 1604 (m), 1493 (w), 1443 (w), 1317 (w), 1302 (w), 1189 (m), 1167 (s), 1091 (vs), 1023 (s), 998 (s), 953 (vs), 914 (s), 870 (m), 715 (m), 695 (m), 648 (m), 638 (s); UV-Vis spectrum: λ_{max} = 768 nm; EA: ($C_2H_6Cl_2CuN_{10}$, 304.59): calcd: C 7.89, H 1.99, N 45.99 %; found: C 8.13, H 2.17, N 45.75 %; BAM drophammer: 3 J; friction tester: 60 N; ESD: 50 mJ (at grain size < 100 μm).

$[Cu(NO_3)_2(1\text{-}AT)_3]$ (9)

A solution of ligand **1** (63.8 mg, 0.75 mmol) in water (2 mL) was slowly added to an aqueous solution (1 mL) of $Cu(NO_3)_2 \cdot 3\ H_2O$ (60.4 mg, 0.25 mmol). Within five days, **9** was obtained in the form of dark blue single crystals suitable for X-ray diffraction. Yield: 88.1 mg (0.20 mmol, 79 %).

DTA (5 °C min^{-1}) onset: 161 °C (exothermic); IR (ATR, cm^{-1}) $\tilde{\nu}$ = 3324 (m), 3275 (w), 3219 (m), 3172 (m), 3151 (m), 3137 (m), 1620 (w), 1597 (w), 1491 (m), 1472 (s), 1436 (m), 1299 (s), 1278 (vs), 1192 (s), 1114 (m), 1095 (s), 1046 (m), 1031 (m), 1001 (s), 966 (s), 936 (m), 898 (m), 886 (m), 846 (m), 809 (m), 748 (m), 722 (w), 717 (w), 702 (m), 649 (s), 641 (s); UV-Vis spectrum: λ_{max} = 686 nm; EA: ($C_3H_9CuN_{17}O_6$, 442.77): calcd: C 8.14, H 2.05, N 53.78 %; found: C 8.48, H 2.09, N 50.95 %; ball drop impact tester: 6 mJ; BAM drophammer: 3 J; friction tester: 2.25 N; ESD: 10 mJ (at grain size < 100 μm).

$[Zn(1\text{-}AT)_6](NO_3)_2$ (12)

An ethanolic solution (0.5 mL) of zinc(II) nitrate hexahydrate (37.2 mg, 125 μmol) was treated with the nitrogen-rich ligand **1** (63.5 mg, 0.75 mmol) dissolved in ethanol (0.5 mL) and mechanically stirred at room temperature for several minutes. After leaving the reaction mixture for crystallization, colorless blocks of **12** suitable for X-ray determination could be collected within three days. The product was filtered off, washed and dried in air. Yield: 34.0 mg (0.05 mmol, 39 %).

DTA (5 °C min^{-1}) onset: 115 °C (endothermic), 180 °C (exothermic); TGA (5 °C min^{-1}): 115–180 °C (loss of coordinating 1-AT ligands), 180 °C (dec.); IR (ATR, cm^{-1}): $\tilde{\nu}$ = 3339 (m), 3312

(m), 3272 (m), 3198 (m), 3179 (m), 3136 (m), 3126 (m), 3104 (m), 3000 (w), 1639 (m), 1617 (m), 1508 (w), 1438 (m), 1383 (s), 1339 (vs), 1321 (vs), 1196 (s), 1129 (m), 1094 (vs), 1045 (w), 988 (s), 966 (s), 889 (s), 829 (m), 721 (m), 701 (m), 643 (vs); EA ($C_6H_{18}N_{32}O_6Zn$, 699.89): calcd: C 10.30, H 2.59, N 64.05 %; found: C 10.80, H 2.57, N 64.67 %; BAM drophammer: < 1 J; friction tester: 6 N; ESD: 620 mJ (at grain size 100–500 μm).

[Cu(μ-Cl)$_2$(2-AT)$_2$] (16)

The copper(II) chloride complex **16** was synthesized through slow addition of an aqueous solution (2 mL) of 2-amino-5*H*-tetrazole (**2**, 42.5 mg, 0.50 mmol) to $CuCl_2 \cdot 2\ H_2O$ (42.6 mg, 0.25 mmol) dissolved in water (1 mL) followed by 10 minutes of stirring mechanically. The desired compound [Cu(μ-Cl)$_2$(2-AT)$_2$] (**16**) was isolated after two days in the form of green blocks suitable for X-ray diffraction. Yield: 31.1 mg (0.10 mmol, 40 %).

DTA (5 °C min^{-1}) onset: 171 °C (exothermic); IR (ATR, cm^{-1}): $\tilde{\nu}$ = 3300 (s), 3248 (m), 3190 (m), 3150 (s), 3011 (w), 2959 (w), 1808 (w), 1611 (m), 1576 (w), 1455 (m), 1395 (w), 1357 (w), 1302 (m), 1210 (m), 1196 (m), 1132 (vs), 1027 (s), 904 (vs), 733 (m), 693 (s), 669 (s); UV-Vis spectrum: λ_{max} = 796 nm; EA ($C_2H_6Cl_2CuN_{10}$, 304.59): calcd: C 7.89, H 1.99, N 45.99 %; found: C 8.16, H 2.04, N 45.90 %; BAM drophammer: < 2 J; friction tester: 40 N; ESD: 10 mJ (at grain size < 100 μm).

[Cu(NO$_3$)$_2$(μ-2-AT)$_2$] (17)

Copper(II) nitrate trihydrate (60.4 mg, 0.25 mmol) was dissolved in water (1 mL). While stirring mechanically, an aqueous solution (2 mL) of the *N*2-subsituted ligand **2** (42.5 mg, 0.50 mmol) was added slowly. The very sensitive nitrate complex **17** was obtained over a period

of three days in the form of blue plates suitable for X-ray diffraction. Yield: 65.3 mg (0.18 mmol, 72 %).

DTA (5 °C min^{-1}) onset: 157 °C (exothermic); IR (ATR, cm^{-1}): $\tilde{\nu}$ = 3255 (m), 3200 (m), 3148 (m), 3125 (m), 2985 (w), 2905 (w), 1579 (w), 1505 (w), 1438 (s), 1408 (m), 1317 (s), 1291 (vs), 1200 (m), 1144 (s), 1045 (s), 1022 (s), 918 (s), 828 (w), 808 (s), 735 (w), 719 (m), 693 (m), 685 (s); UV-Vis spectrum: λ_{max} = 689 nm; EA ($C_2H_6CuN_{12}O_6$, 357.70): calcd: C 6.72, H 1.69, N 46.99 %; found: C 6.89, H 1.76, N 47.03 %; BAM drophammer: < 1 J; friction tester: 2 N; ESD: 10 mJ (at grain size < 100 μm).

$[Cu(H_2O)_2(2\text{-}AT)_4](ClO_4)_2$ (18)

To an aqueous solution (1 mL) of the nitrogen-rich compound **2** (213 mg, 2.50 mmol), a solution of copper(II) perchlorate hexahydrate was added dropwise (92.6 mg, 0.25 mmol). After three days, coordination compound **18**, an extremely sensitive complex, was isolated in the form of blue blocks suitable for X-ray diffraction. Yield: 82.1 mg (0.13 mmol, 52 %).

DTA (5 °C min^{-1}) onset: 110 °C (endothermic), 173 °C (exothermic); IR (ATR, cm^{-1}): $\tilde{\nu}$ = 3485 (w), 3443 (w), 3283 (m), 3248 (m), 3173 (m), 3000 (vw), 1626 (w), 1608 (m), 1572 (vw), 1490 (vw), 1396 (w), 1312 (m), 1176 (w), 1153 (m), 1054 (vs), 1029 (vs), 936 (m), 899 (s), 732 (w), 693 (w), 678 (s), 620 (s); UV-Vis spectrum: λ_{max} = 647 nm; EA ($C_4H_{16}Cl_2CuN_{20}O_{10}$, 638.75): calcd: C 7.52, H 2.52, N 43.86 %; found: C 8.10, H 2.39, N 43.78 %; BAM drophammer: 1 J; friction tester: 0.4 N; ESD: 10 mJ (at grain size 100–500 μm).

General procedure for the preparation of the metal(II) (Fe^{II}, Zn^{II}) 2-AT perchlorate coordination compounds (19/20):

While stirring mechanically, a solution of 2-amino-5*H*-tetrazole (**2**, 106 mg, 1.25 mmol) in water (2 mL) was slowly added to an aqueous solution (1 mL) of the corresponding metal(II) perchlorate (**19**: $Fe(ClO_4)_2 \cdot 6\ H_2O$ (63.7 mg, 0.25 mmol), **20**: $Zn(ClO_4)_2 \cdot 6\ H_2O$ (93.1 mg, 0.25 mmol)) at room temperature. The reaction mixtures were left for crystallization until a crystalline material appeared. The products obtained were filtered off, washed and dried in air.

$[Fe(H_2O)(2\text{-}AT)_5](ClO_4)_2$ (19)

Colorless blocks of **19**, which were suitable for X-ray analysis started to crystallize within two days. Yield: 82.0 mg (0.12 mmol, 48 %).

DTA (5 °C min^{-1}) onset: 159 °C (exothermic); IR (ATR, cm^{-1}): $\tilde{\nu}$ = 3262 (w), 3152 (m), 1664 (w), 1601 (w), 1502 (vw), 1453 (vw), 1389 (w), 1304 (m), 1285 (vw), 1238 (vw), 1151 (m), 1144 (m), 1080 (vs), 1041 (s), 1026 (s), 944 (m), 935 (m), 912 (m), 894 (m), 717 (w), 694 (m), 680 (m), 674 (m), 621 (vs); UV-Vis spectrum: λ_{max} = 868 nm; EA ($C_5H_{17}Cl_2FeN_{25}O_9$, 698.10): calcd: C 8.60, H 2.45, N 50.16 %; found: C 9.10, H 2.52, N 49.55 %; BAM drophammer: 1.5 J; friction tester: 0.15 N; ESD: 10 mJ (at grain size 100–500 μm).

$[Zn(H_2O)(2\text{-}AT)_5](ClO_4)_2$ (20)

After two days, **20** was obtained in the form of colorless blocks suitable for X-ray diffraction. Yield: 110 mg (0.16 mmol, 64 %).

DTA (5 °C min^{-1}) onset: 132 °C (endothermic), 200 °C (exothermic); IR (ATR, cm−1): $\tilde{\nu}$ = 3340 (m), 3261 (m), 3175 (m), 3156 (m), 3004 (w), 1660 (w), 1634 (w), 1600 (m), 1573 (w), 1505 (vw), 1454 (w), 1404 (w), 1340 (vw), 1306 (m), 1240 (w), 1194 (w), 1176 (w), 1155 (m),

1145 (m), 1076 (vs), 1050 (s), 1034 (s), 1026 (s), 935 (m), 895 (s), 758 (vw), 718 (w), 694 (m), 680 (m), 646 (m), 620 (s); EA: ($C_5H_{17}Cl_2N_{25}O_9Zn$, 707.64): calcd: C 8.49, H 2.42, N 49.49 %; found: C 8.99, H 2.67, N 49.15 %; BAM drophammer: 1.5 J; friction tester: 0.5 N; ESD: 10 mJ (at grain size < 100 μm).

General procedure for the preparation of the metal(II) (Fe^{II}, Zn^{II}, Cu^{II}) 2-AT perchlorate coordination compounds (21–23) with cocrystallized 2-ATs:

The relevant metal(II) perchlorate salt (**21**: iron(II) perchlorate hexahydrate (63.7 mg, 0.25 mmol), **22**: zinc(II) perchlorate hexahydrate (93.1 mg, 0.25 mmol), **23**: copper(II) perchlorate hexahydrate (92.6 mg, 0.25 mmol)) were dissolved in the minimum amount of distilled water or ethanol in the case of complex **23**. An aqueous or ethanolic (in case of **23**) solution (1 mL) of the energetic tetrazole ligand **2** (213 mg, 2.50 mmol) was added, the reaction mixture mechanically stirred for one minute and finally left for crystallization. After crystallization, the cocrystallized species were filtered off, washed with cold ethanol and dried in air.

$[Fe(2\text{-}AT)_6](ClO_4)_2 \cdot 2\text{-}AT$ (21)

Product **21** was obtained after four days in the form of colorless blocks suitable for X-ray diffraction. Yield: 41.1 mg (0.04 mmol, 16 %).

DTA (5 °C min^{-1}) onset: 106 °C (endothermic), 169 °C (exothermic); IR (ATR, cm^{-1}): $\tilde{\nu}$ = 3329 (m), 3265 (m), 3152 (m), 3139 (m), 1602 (m), 1503 (vw), 1461 (w), 1388 (w), 1304 (m), 1286 (w), 1231 (w), 1145 (m), 1084 (vs), 1041 (s), 1026 (s), 1014 (s), 940 (s), 913 (m), 897 (s), 891 (s), 881 (m), 724 (m), 703 (m), 695 (m), 682 (m), 673 (m), 622 (s); UV-Vis spectrum: λ_{max} = 795 nm; EA: ($C_8H_{24}Cl_2FeN_{40}O_8$, 935.30): calcd: C 10.27, H 2.59, N 59.90 %; found: C 10.84,

H 2.62, N 59.71 %; BAM drophammer: < 1 J; friction tester: 0.1 N; ESD: 25 mJ (at grain size 100–500 μm).

$[Zn(2\text{-}AT)_6](ClO_4)_2 \cdot 2\text{-}AT$ (22)

Within four days, complex **22** crystallized in the form of colorless plates suitable for X-ray diffraction. Yield: 46.0 mg (0.05 mmol, 20 %).

DTA (5 °C min^{-1}) onset: 96 °C (endothermic), 192 °C (exothermic); IR (ATR, cm^{-1}): $\tilde{\nu}$ = 3329 (m), 3263 (m), 3171 (m), 3152 (m), 3139 (m), 3005 (vw), 1602 (m), 1503 (vw), 1460 (w), 1409 (w), 1388 (w), 1305 (m), 1286 (w), 1228 (w), 1182 (w), 1145 (m), 1086 (vs), 1041 (s), 1027 (s), 1013 (s), 940 (s), 912 (s), 898 (s), 890 (s), 880 (s), 724 (m), 718 (m), 703 (m), 695 (m), 680 (m), 673 (m), 622 (s); EA: ($C_8H_{24}Cl_2N_{40}O_8Zn$, 944.83): calcd: C 10.17, H 2.56, N 59.30 %; found: C 10.42, H 2.57, N 59.10 %; BAM drophammer: 2 J; friction tester: 0.2 N; ESD: 30 mJ (at grain size 100–500 μm).

$[Cu(2\text{-}AT)_6](ClO_4)_2 \cdot 2\text{-}AT$ (23)

Within one hour, complex **23** appeared in the form of blue blocks suitable for X-ray diffraction. Yield: 30.0 mg (0.03 mmol, 13 %).

DTA (5 °C min^{-1}) onset: 108 °C (endothermic), 157 °C (exothermic); IR (ATR, cm^{-1}): $\tilde{\nu}$ = 3354 (m), 3319 (m), 3281 (m), 3268 (m), 3256 (m), 3244 (m), 3227 (m), 3176 (m), 3142 (m), 1612 (m), 1458 (w), 1393 (w), 1320 (w), 1302 (w), 1293 (m), 1223 (m), 1197 (w), 1188 (w), 1148 (m), 1098 (vs), 1060 (s), 1047 (s), 1024 (vs), 1015 (s), 948 (s), 932 (s), 901 (s), 889 (s), 726 (m), 705 (s), 681 (m), 674 (m), 668 (m), 622 (vs), 473 (w), 454 (m); UV-Vis spectrum:

λ_{max} = 655 nm; EA: ($C_8H_{24}Cl_2CuN_{40}O_8$, 943.00): calcd: C 10.19, H 2.57, N 59.41 %; found: C 10.23, H 2.51, N 59.41 %; BAM drophammer: 1 J; friction tester: < 0.2 N; ESD: 1.2 mJ (at grain size 100–500 μm).

12. References

S1 CrysAlisPRO (Version 171.33.41), Oxford Diffraction Ltd., 2009.

S2 A. Altomare, G. Cascarano, C. Giacovazzo, and A. Guagliardi, *J. Appl. Crystallogr.*, 1992, **26**, 343.

S3 a) A. Altomare, G. Cascarano, C. Giacovazzo, A. Guagliardi, A. G. G. Moliterni, M. C. Burla, G. Polidori, M. Camalli and R. Spagna, SIR97, 2003; b) A. Altomare, M. C. Burla, M. Camalli, G. L. Cascarano, C. Giacovazzo, A. Guagliardi, A. G. G. Moliterni, G. Polidori and R. Spagna, *J. Appl. Crystallogr.*, 1999, **32**, 115.

S4 a) G. M. Sheldrick, SHELXL-97, University of Göttingen, Germany, 1997; b) G. M. Sheldrick, *Acta Crystallogr. Sect. A*, 2008, **64**, 112.

S5 A. L. Spek, PLATON, Utrecht University, The Netherlands, 1999.

S6 L.J. Farrugia, *J. Appl. Cryst.*, 2012, **45**, 849.

S7 Empirical absorption correction using spherical harmonics, implemented in SCALE3 ABSPACK scaling algorithm (CrysAlisPro Oxford Diffraction Ltd., Version 171.33.41, 2009).

S8 APEX3, Bruker AXS Inc., Madison, Wisconsin, USA.

S9 J. R. Rodriguez-Carvajal, Abstracts of the Satellite Meeting on Powder Diffration of XV Congress of the IUCr, Toulouse, France, 1990, 127.

S10 NATO standardization agreement (STANAG) on explosives, impact sensitivity tests, no. 4489, 1st ed., Sept. 17, 1999.

S11 WIWEB-Standardarbeitsanweisung 4-5.1.02, Ermittlung der Explosionsgefährlichkeit, hier der Schlagempfindlichkeit mit dem Fallhammer, Nov. 8, 2002.

S12 OZM, http://www.ozm.cz, (accessed April 2018).

S13 BAM, http://www.bam.de, (accessed April 2018).

S14 Military Standard 1751A (MIL-STD-1751A): safety and performance tests for qualification of explosives (high explosives, propellants and pyrotechnics), method 1016, Dec. 11, 2001.

S15 UN Model Regulation: Recommendations on the Transport of Dangerous Goods – Manual of Tests and Criteria, section 13.4.2.3.3, 2015.

S16 NATO standardization agreement (STANAG) on explosive, friction sensitivity tests, no. 4487, 1st ed., Aug. 22, 2002.

S17 WIWEB-Standardarbeitsanweisung 4-5.1.03, Ermittlung der Explosionsgefährlichkeit oder der Reibeempfindlichkeit mit dem Reibeapparat, Nov. 8, 2002.

S18 Impact: insensitive > 40 J, less sensitive ≥ 35 J, sensitive ≥ 4 J, very sensitive ≤ 3 J; Friction: insensitive > 360 N, less sensitive = 360 N, sensitive < 360 N and > 80 N, very sensitive ≤ 80 N, extremely sensitive ≤ 10 N. According to the UN Recommendations on the Transport of Dangerous Goods, (+) indicates not safe for transport.

S19 R. Scharf, PhD thesis, Ludwig-Maximilians Universität München, 2016.

S20 T. M. Klapötke, D. G. Piercey, J. Stierstorfer, *Dalton Trans.* 2012, **41**, 9451.